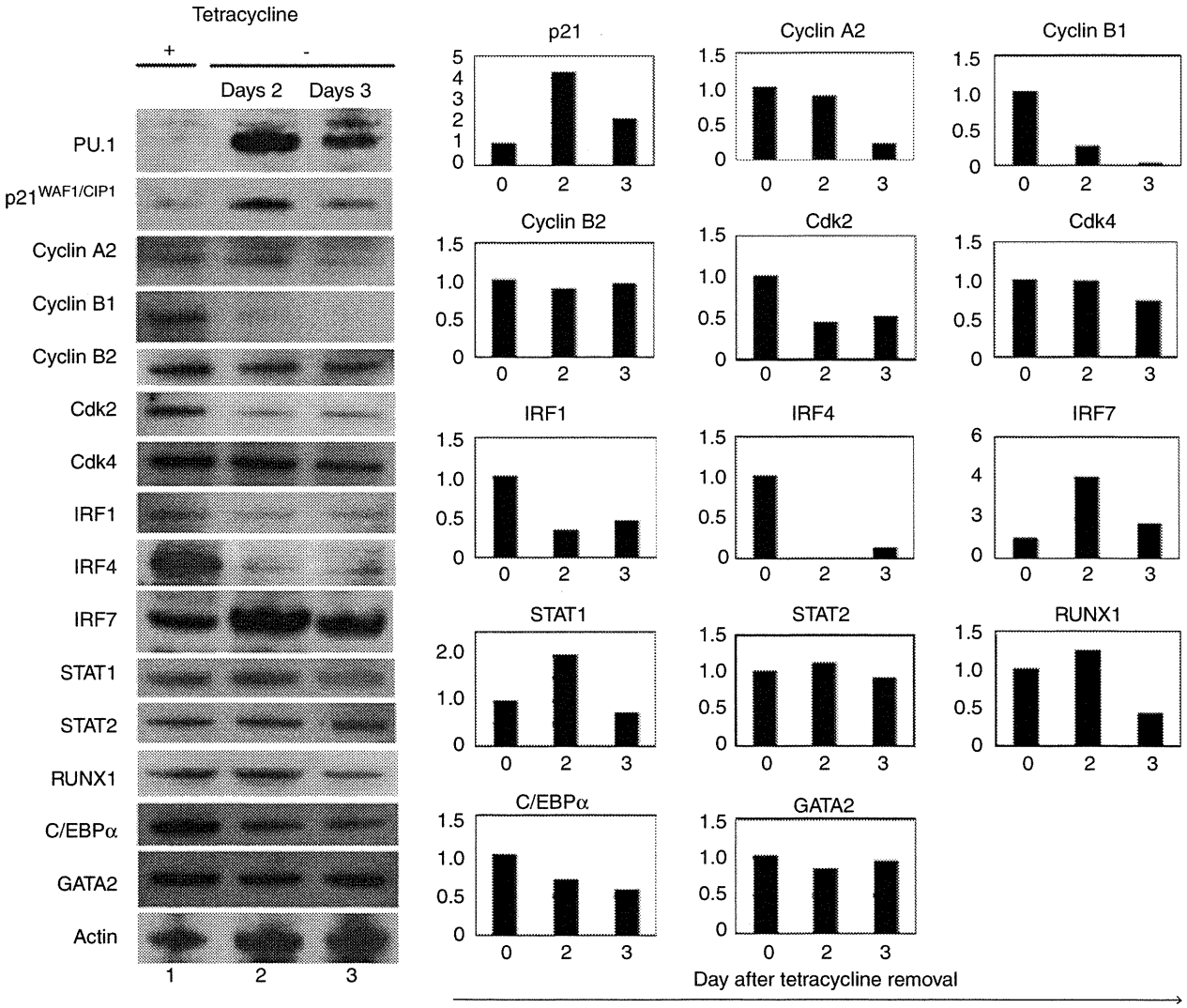

Figure 1 The IRF7 and p21$^{WAF1/CIP}$ were upregulated and IRF4 was downregulated in U266$^{tetPU.1}$ cells after PU.1 induction. Western blotting analyses of cell cycle-related genes, IRFs, STATs and transcription factor essential for hematopoiesis were performed on cell extracts of U266$^{tetPU.1}$ cells before (lane 1) and at day 2 (lane 2) and day 3 (lane 3) after PU.1 induction by removal of tetracycline. Right panels are based on the densitometry of the left panel. Each expression level of day 0 is set as 1, and relative expression levels at day 2 and 3 were shown in each right panel.

expressing PU.1, PU.1 also bound to the *TRAIL* promoter (Figure 4b). Therefore, we evaluated the *TRAIL* promoter to search for transcription-binding sites and found one potential PU.1-binding site located in 30-bp 3′-downstream of the transcription start site (Figure 5a). We performed electromobility shift assays using oligonucleotides harboring the potential PU.1-binding site and nuclear extracts of U266$^{tetPU.1}$ cells and identified several bands for protein binding (Figure 5b). Competition with CD11b promoter oligonucleotides including the PU.1-binding site and addition of the anti-PU.1 antibody eliminated one band for protein binding (Figure 5b, lanes 4 and 5) of the oligonucleotides for the 30-bp 3′-downstream region of the transcription start site (Figure 5a), indicating that the binding to the oligonucleotides was PU.1 specific. We also identified the same PU.1-binding complex with the same oligonucleotides and nuclear extracts of KMS12PE$^{tetPU.1}$ cells expressing PU.1 (Figure 5c). In addition, *in vitro*-translated PU.1 protein bound to the same oligonucleotides and CD11b oligonucleotides and the anti-PU.1 antibody eliminated the binding (Figure 5d, lanes 1–5), indicating that PU.1 binds to the oligonucleotides. Next we introduced mutations into the PU.1-binding site (GAGA to TCGC) in the oligonucleotides and performed electromobility shift assays. We detected two major shifted bands, but these did not disappear after competition with the CD11b oligonucleotides or addition of the anti-PU.1 antibody (Figure 5d, lanes 6–10), indicating that the mutations in the PU.1-binding motif completely abolished PU.1 binding to the *TRAIL* promoter region. Therefore, these data indicate that PU.1 binds to the 30-bp 3′-downstream region of the transcription start site of the *TRAIL* promoter.

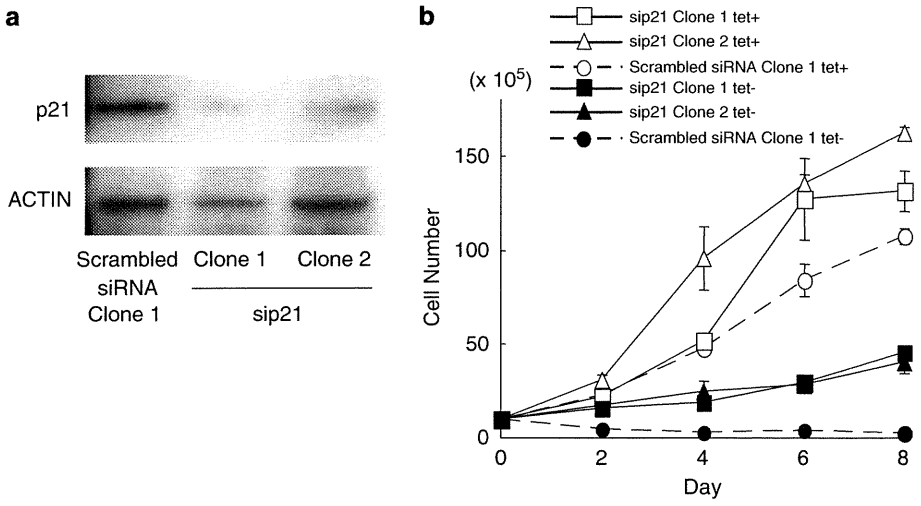

Figure 2 Growth arrest of U266$^{tetPU.1}$ cells expressing PU.1 may be partially induced by upregulated p21. (**a**) The protein levels of p21 were strongly suppressed by stably expressed small interference RNA (siRNA) for p21. Western blot analysis of p21 at day 2 after PU.1 induction in U266$^{tetPU.1}$ derivative cell lines expressing siRNA for p21 or its scramble was shown. (**b**) Growth curve of two U266$^{tetPU.1}$ derivative cell lines expressing siRNA for p21 with (open triangle and open square) or without tetracycline (closed triangle and closed square) and one U266$^{tetPU.1}$ derivative cell line expressing scrambled siRNA with (open circle) or without tetracycline (closed circle). Error bars represent the s.d. derived from three independent experiments.

PU.1 directly transactivates the TRAIL promoter in U266$^{tetPU.1}$ and KMS12PE$^{tetPU.1}$ cells

To evaluate whether the binding of PU.1 can directly transactivate the *TRAIL* promoter, we performed luciferase reporter assays with a construct comprised of the *TRAIL* promoter and a luciferase reporter gene in U266$^{tetPU.1}$ and KMS12PE$^{tetPU.1}$ cells before and after PU.1 induction (Figure 6a). With the wild-type *TRAIL* promoter, the expression level was upregulated by 70-fold in U266$^{tetPU.1}$ cells and 26-fold in KMS12PE$^{tetPU.1}$ cells compared with that of pGL4.26 alone when tetracycline was not removed (without PU.1 expression) (Figures 6b and c). In addition, when PU.1 was upregulated, reporter gene expression was highly upregulated by 4.6-fold compared with that with no PU.1 expression in U266$^{tetPU.1}$ cells, and 6.6-fold in KMS12PE$^{tetPU.1}$ cells. We further examined whether the upregulated reporter gene expression was dependent on PU.1 binding to the *TRAIL* promoter. To achieve this, we introduced the same mutations (GAGA to TCGC) into the PU.1-binding site in the 30-bp 3′-downstream region of the transcription start site of the *TRAIL* promoter construct that were shown to abolish PU.1 binding in electromobility shift assays (Figure 5d), and found that these mutations completely eliminated the upregulation of reporter gene expression relative to the control plasmid (pGL4.26) in both U266$^{tetPU.1}$ and KMS12PE$^{tetPU.1}$ cells regardless of whether or not PU.1 was induced (Figures 6b and c). Taken together, these data suggest that TRAIL expression in both U266$^{tetPU.1}$ and KMS12PE$^{tetPU.1}$ cells expressing PU.1 is highly dependent on direct binding of PU.1 to the *TRAIL* promoter.

Discussion

We earlier reported that downregulation of PU.1 in myeloma cells is necessary for their growth and survival, and that conditional expression of PU.1 in myeloma cells induced growth arrest and apoptosis (Tatetsu *et al.*, 2007). In this study, we analysed the genes involved in the growth arrest and apoptosis of U266 myeloma cells by performing DNA microarray analyses and comparing the gene expressions before and after PU.1 induction. We found that among cell cycle-related genes, p21 was upregulated and cyclin A2, cyclin B1, CDK2 and CDK4 were downregulated after PU.1 induction. Among apoptosis-related genes, TRAIL was directly transactivated by PU.1 and induced apoptosis in both U266$^{tetPU.1}$ and KMS12PE$^{tetPU.1}$ cells expressing PU.1.

After PU.1 induction, many cyclins and CDKs were downregulated, and these findings are compatible with the growth arrest of U266 cells. In contrast, among tumor suppressor genes, only p21 was upregulated after PU.1 induction, and this was confirmed at the protein level. Given the fact that knockdown of p21 by siRNA partially rescue the PU.1-induced growth arrest of U266$^{tetPU.1}$ cells, p21 may partially mediate the induction of growth arrest of myeloma cells by PU.1. The mechanism of the upregulation of p21 after PU.1 induction in U266$^{tetPU.1}$ cells is now being elucidated. It was reported that IRF1 directly transactivates p21 gene expression by binding to the p21 gene promoter (Coccia *et al.*, 1999). Among the IRF family members, IRF7 and IRF9 were highly upregulated at 24.8-fold and 3.9-fold in mRNA levels, respectively. It is reasonable that these IRFs may induce p21 expression after PU.1 induction.

We also evaluated the gene expression levels of apoptosis-related genes in U266 cells expressing PU.1 and found that TRAIL was highly upregulated after PU.1 induction and stably expressed siRNAs for TRAIL suppressed the apoptosis of not only U266$^{tetPU.1}$ but also KMS12PE$^{tetPU.1}$ cells expressing PU.1. It is likely that TRAIL is a key molecule for inducing apoptosis in U266$^{tetPU.1}$ and KMS12PE$^{tetPU.1}$ cells after

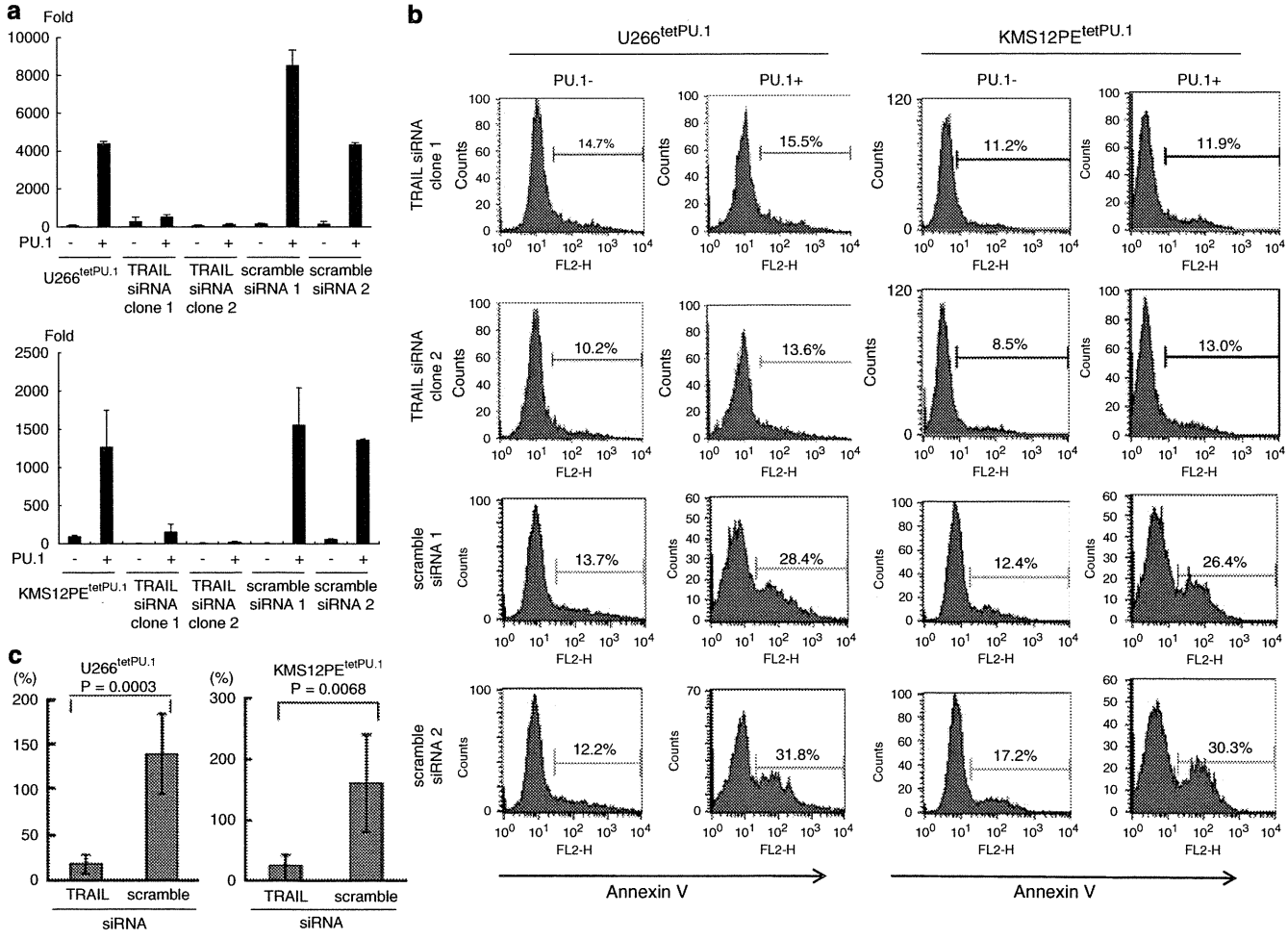

Figure 3 Apoptosis of U266$^{tetPU.1}$ and KMS12PE$^{tetPU.1}$ cells expressing PU.1 may be highly induced by upregulated tumor necrosis factor (TNF)-related apoptosis inducing ligand (TRAIL). (**a**) TRAIL is upregulated in U266$^{tetPU.1}$ (upper panel) and KMS12PE$^{tetPU.1}$ cells (lower panel) after PU.1 induction. Real-time PCR of TRAIL was performed for U266$^{tetPU.1}$ and KMS12PE$^{tetPU.1}$ cells and their transformants stably expressing small interference RNAs (siRNAs) for TRAIL or its scrambled sequences. Bar graphs represent the mean and s.d. of three experiments. (**b**) The siRNAs for TRAIL inhibit apoptosis of U266$^{tetPU.1}$ and KMS12PE$^{tetPU.1}$ cells expressing PU.1. After conditional expression of PU.1, Annexin V-positive cells of U266$^{tetPU.1}$ and KMS12PE$^{tetPU.1}$ cells stably expressing siRNA for TRAIL or its scrambles were determined as apoptotic cells. (**c**) Suppression of apoptosis by siRNA for TRAIL is statistically significant. On the basis of the results of Annexin V staining as shown in Figure 3b, percentage of increases of apoptotic cells in U266$^{tetPU.1}$ and KMS12PE$^{tetPU.1}$ cells stably expressing siRNA for TRAIL or its scrambles after PU.1 induction are shown compared with those before PU.1 induction (set as 100%). Means ± s.d. for three independent clones expressing siRNA for TRAIL or its scrambled siRNA are shown.

PU.1 expression, because it was found to effectively induce apoptosis in multiple myeloma cells *in vitro* (Mariani *et al.*, 1997; Gazitt, 1999; Mitsiades *et al.*, 2001, 2002). We further found that PU.1 itself directly transactivates the *TRAIL* promoter in both myeloma cell lines. This is a first report to show that PU.1 is a direct transactivator of *TRAIL* gene expression. From this aspect, PU.1 may be a regulator of unlimited proliferation of hematopoietic cells including plasma cells through upregulation of the cell death inducer TRAIL.

As shown in Figures 3b and c, siRNA for TRAIL may not completely suppress apoptosis of U266$^{tetPU.1}$ and KMS12PE$^{tetPU.1}$ cells after PU.1 expression, suggesting that other factors may be involved in the apoptosis of these cells. IRF4 is an essential transcription factor for generation of plasma cells, because transgenic mice with a conditional knockout of Irf4 in germinal center B cells were unable to differentiate memory B cells into plasma cells (Klein *et al.*, 2006). In addition, it was reported that knockdown of IRF4-induced apoptosis in many genetic types of myeloma cells (Shaffer *et al.*, 2008). Therefore, because protein levels of IRF4 were strongly downregulated to 0.02-fold at 2 days and 0.18-fold 3 days after PU.1 induction (Figure 1), it is possible that this downregulation of IRF4 may also induce apoptosis in myeloma cells after PU.1 expression.

In this study, we found that PU.1 can directly transactivate *TRAIL* gene expression in myeloma cells. This finding may be universal for all hematopoietic cells, although we still need to analyse whether PU.1 also induces *TRAIL* gene expression in other hematopoietic

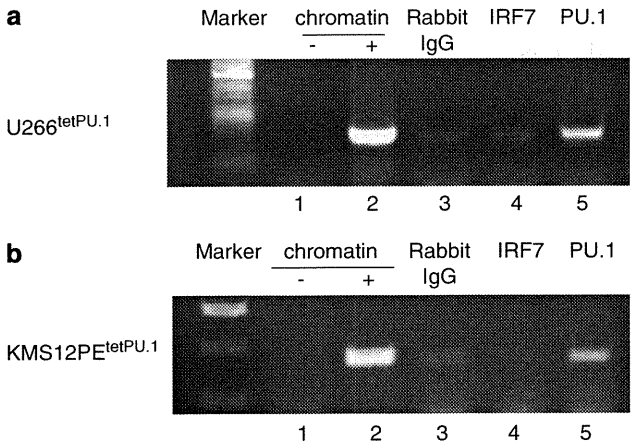

Figure 4 The PU.1 binds to the *TRAIL* promoter region in both U266$^{tetPU.1}$ and KMS12PE$^{tetPU.1}$ cells *in vivo*. (**a**) and (**b**) Chromatin immunoprecipitation (ChIP) assays reveal that PU.1, but not IRF7, binds to the *TRAIL* promoter region. ChIP assays were performed on U266$^{tetPU.1}$ (**a**) and KMS12PE$^{tetPU.1}$ cells (**b**) at 1 day after PU.1 induction. Chromatin DNA was immunoprecipitated with anti-IRF7 or anti-PU.1 antibodies, or rabbit IgG as a control. After extraction of genomic DNA, PCR amplification of the *TRAIL* promoter and exon 1 region was performed using water (lane 1), input chromatin DNA (lane 2) or genomic DNA immunoprecipitated by rabbit IgG (lane 3), anti-IRF7 antibody (lane 4) or anti-PU.1 antibody (lane 5).

lineages. If this proves to be the case, upregulation of PU.1 may be a universal therapeutic molecular target for hematopoietic malignancies. Indeed, upregulation of TRAIL may represent a major target for HDAC inhibitors (Insinga *et al.*, 2005; Nebbioso *et al.*, 2005), and this could be mediated by upregulation of PU.1. The PU.1 also induced downregulation of IRF4 that may result in apoptosis of myeloma cells (Shaffer *et al.*, 2008). Therefore, upregulation of PU.1 may represent a possible treatment of multiple myeloma by inducing the combination of upregulation of TRAIL and downregulation of IRF4.

Materials and methods

DNA microarray analysis
We earlier generated U266$^{tetPU.1}$ and KMS12PE$^{tetPU.1}$ cells that express PU.1 by tet-off system (Tatetsu *et al.*, 2007). At first, RNA was extracted from U266$^{tetPU.1}$ cells at three different time points, before, and 1 or 3 days after tetracycline removal. To compare gene expression differences between before and after tetracycline removal, the microarray analysis was performed using Illumina:Sentrix Human-6 Expression BeadChip as recommended by the manufacturer. Expression levels of genes were analysed by GeneSpring 7.2 software.

Cell culture
Human myeloma cell line U266$^{tetPU.1}$ and KMS12PE$^{tetPU.1}$ cells, and their derivatives were grown in RPMI 1640 containing 10% fetal bovine serum at 37 °C.

Western blot analysis
The cell lysates were separated by sodium dodecyl sulfate–polyacrylamide gel electrophoresis and transferred onto nitrocellulose membranes. The membranes were incubated with anti-PU.1, anti-p21$^{WAF/CIP1}$, anti-cyclin A2, anti-cyclin B2, anti-CDK2, anti-CDK4, anti-IRF1, anti-IRF4, anti-IRF7, anti-STAT1, anti-STAT2, anti-RUNX1, anti-C/EBPα, anti-GATA1, anti-GATA2, anti-Actin primary antibody (Santa Cruz Biotechnology, Santa Cruz, CA, USA) or anti-cyclin B1 (Abcam, Cambridge, MA, USA) for 3–16 h. Finally, the membranes were incubated with peroxidase-labeled secondary antibodies for 1 h, and developed using an enhanced chemiluminescence system (Amersham Life Science Inc., Arlington Heights, IL, USA).

Generation of U266$^{tetPU.1}$ and KMS12PE$^{tetPU.1}$ cells stably expressing siRNA for TRAIL or p21 and those scrambled siRNAs
The siRNA expression vectors were generated by insertion of annealed oligonucleotides for TRAIL or p21 and those scrambled siRNAs into from *BamHI* to *HindIII* site of pRNA-U6.1/Zeo or pRNA-U6.1/Hygro (GenScript, Piscataway, NJ, USA) (Supplementary Information). These siRNA expression vectors were transfected to U266$^{tetPU.1}$ or KMS12PE$^{tetPU.1}$ cells by elecrotoporation and stable transformants were obtained by zeocin or hygromycin selection.

Real-time PCR
Quantitative Taqman PCR was performed using commercially available assay on demand probe primer sets for TRAIL and β-actin (Applied Biosystems, Foster City, CA, USA) and Taqman Universal PCR Master Mix reagent using an ABI Prism 7700 Sequence Detection System (Applied Biosystems). The expression levels of β-actin were used to standardize the relative expression levels of TRAIL. The expression level of TRAIL in U266$^{tetPU.1}$ and KMS12PE$^{tetPU.1}$ cells before tetracycline removal was set as 100.

Detection of apoptosis
To detect apoptosis of myeloma cells, the cells were stained with an Annexin V Phycoerythrin Apoptosis Detection kit (Medical and Biological Laboratories, Nagoya, Japan) and analysed for Annexin V expression with FACS caliber (Becton Dickinson, San Jose, CA, USA).

Chromatin immunoprecipitation assay
Chromatin immunoprecipitation assays were performed as described earlier (Okuno *et al.*, 2005). Briefly, 1×10^7 of U266$^{tetPU.1}$ or KMS12PE$^{tetPU.1}$ cells 1 day after tetracycline removal were treated with 0.5% formaldehyde and genomic DNA was extracted and sonicated. Small amount of genomic DNA was saved as input DNA. The total input sample was diluted 1/100 before being used as a template for PCR. Soluble chromatin was treated with anti-PU.1 antibody, anti-IRF7 antibody and rabbit IgG, and immunoprecipitated by protein A agarose beads (Santa Cruz Biotechnology). Each precipitated DNA was eluted and extracted as described earlier and subjected for PCR. PCR was performed using *TRAIL* promoter sense primers, 5′-TGAGGATATGTTAGG GAAAAGCA-3′ located 284-bp upstream of transcription start site, and *TRAIL* exon 1 antisense primer 5′-GATCAC GATCAGCACGCAGGTCT-3′ located 140-bp downstream of transcription start site.

Electromobility shift assay
Nuclear extracts of 5×10^6 U266$^{tetPU.1}$ or KMS12PE$^{tetPU.1}$ cells 1 day after removal of tetracycline were prepared with NE-PER Nuclear and Cytoplasmic Extraction Reagents (Pierce, Rockford, IL, USA). The PU.1 cDNA was subcloned

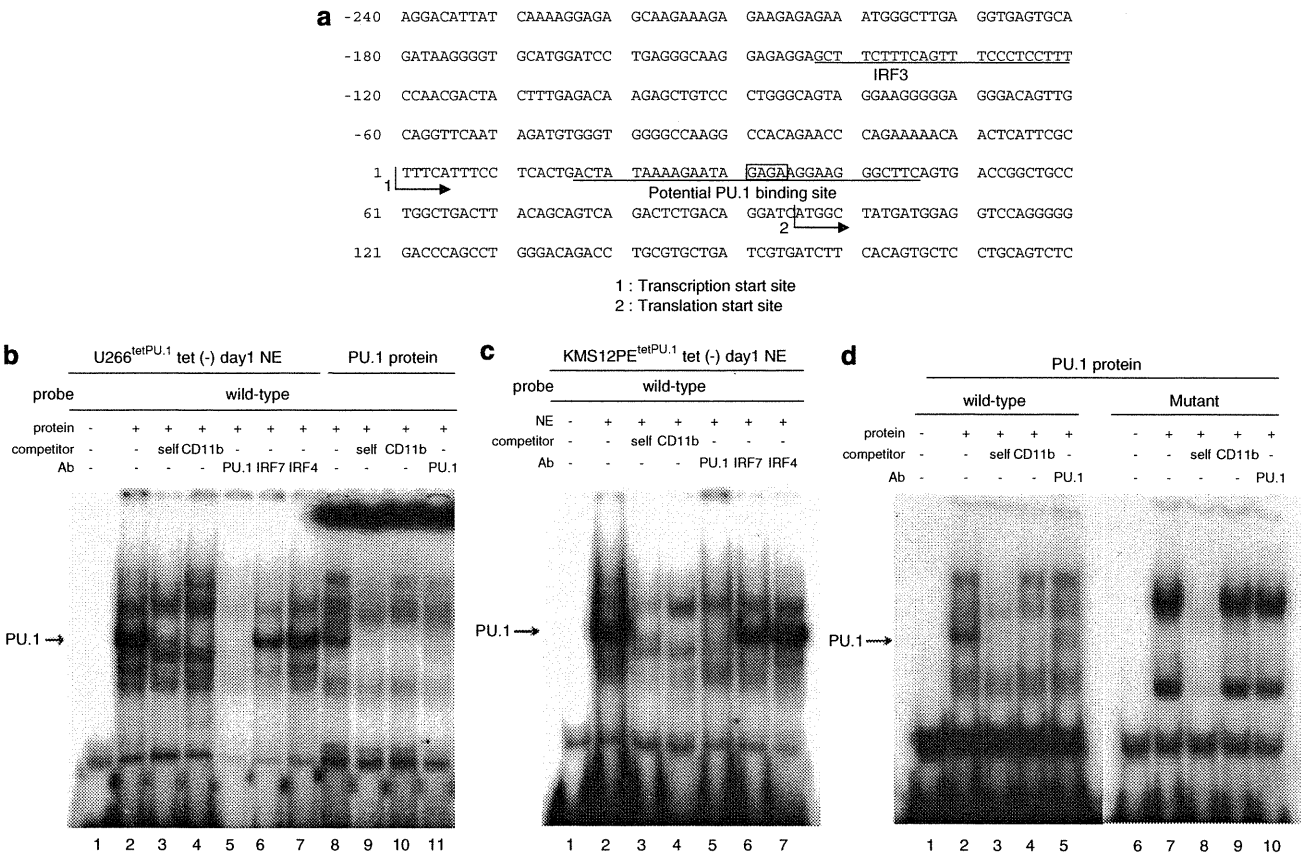

Figure 5 The PU.1 binds to a 30-bp 3′-downstream region of the transcription start site of the *TRAIL* gene. (**a**) A potential PU.1-binding site is located in a 30-bp 3′-downstream region of the transcription start site of the *TRAIL* gene. The sequence of the *TRAIL* promoter region and 180 bp of exon 1 is shown. The potential PU.1-binding site is located in a 30-bp 3′-downstream region of the transcription start site in the 5′-non-coding region of exon 1. The sequence for oligonucleotides used for electromobility shift assay (EMSA) in Figures 5b–d is underlined (wild-type). A earlier described binding site for IRF3 is also shown (Kirshner *et al*., 2005). (**b, c**) PU.1 binds to the 30-bp 3′-downstream region of the transcription start site. An EMSA was performed using nuclear extracts of U266$^{tetPU.1}$ (**b**) and KMS12PE$^{tetPU.1}$ cells (**c**) at day 1 after PU.1 induction and the oligonucleotides shown in Figure 4a (wild-type). 'Self' refers to competition with itself. 'CD11b' refers to competition with oligonucleotides complementary to the CD11b promoter region including the PU.1-binding site (CD11b oligonucleotides). The relative position of the PU.1 complex is shown on the left side of the panels (arrow). The PU.1, IRF7 and IRF4 refer to antibodies used for supershift assays. The anti-PU.1 antibody does not create a supershift but instead eliminates the PU.1 complex (lane 5). *In vitro*-translated PU.1 generated PU.1-specific band as a positive control as shown in (d) (b, lanes 8–11). (**d**) *In vitro*-translated PU.1 protein specifically binds to the 30-bp 3′-downstream region of the transcription start site. EMSAs were performed using *in vitro*-translated PU.1 and wild-type oligonucleotides or mutant oligonucleotides of the PU.1-binding site (GAGA to TCGC). The relative position of the PU.1 complex is shown on the left side of the panels (arrow). The CD11b oligonucleotides and anti-PU.1 antibody eliminate the PU.1 complex (lanes 4 and 5). In contrast to the PU.1 complex with the wild-type oligonucleotides, there is no PU.1 complex with the mutant oligonucleotides that can be diminished by competition with the CD11b oligonucleotides or anti-PU.1 antibody (lanes 7–10).

into pT_NT Vector (Promega, Madison, WI, USA) and subjected to TnT Quick Coupled Transcription/Translation Systems (Promega) to prepare *in vitro*-translated PU.1 protein. Oligonucleotides, 5′-ACTATAAAAGAATAGAGAAGGAA GGGCTTC-3′ and 5′-GAAGCCCTTCCTTCTCTATTCTT TTATAGT-3′, were annealed and subjected to electromobility shift assay for PU.1-binding site in a 30-bp 3′-downstream region of the transcription start site of the *TRAIL* gene, whereas oligonucleotides, 5′-ACTATAAAAGAATATCGC AGGAAGGGCTTC-3′ and 5′-GAAGCCCTTCCTGCGAT ATTCTTTTATAGT-3′ were annealed and used as mutant oligonucleotides for the PU.1-binding site of the *TRAIL* promoter. Annealed oligonucleotides were labeled with [γ-P^{32}]ATP using T4 polynucleotide kinase and incubated with nuclear extracts or *in vitro*-translated PU.1 protein in 10 mM HEPES (pH 7.8), 50 mM KCl, 1 mM dithiothreitol, 1 mM EDTA, and 5% glycerol for 15 min at 0 °C. Reaction mixtures were separated with 6% polyacrylamide gels in 0.5 × TBE buffer at 4 °C. Gels were dried before autoradiography. Anti-PU.1, anti-IRF4 and anti-IRF7 antibodies (Santa Cruz) were used for supershift assays. The CD11b promoter oligonucleotides harboring PU.1-binding site 5′-CTACTTCTCCTTTTCTGCCCTTCTTTG-3′ and 5′-CAAA GAAGGGCAGAAAAGGAGAAGTAG-3′, which have been described earlier (Pahl *et al*., 1993), were annealed and used for competition assays.

Luciferase assay

In total, 1.5 kb DNA fragment consists of the 1480-bp human *TRAIL* promoter and 55-bp of exon 1 5′ non-coding region was amplified with primers 5′-TATACTCGAGGATAG AAGGCAAGGGCAGGAAGT-3′ and 5′-ATATAAGCTT

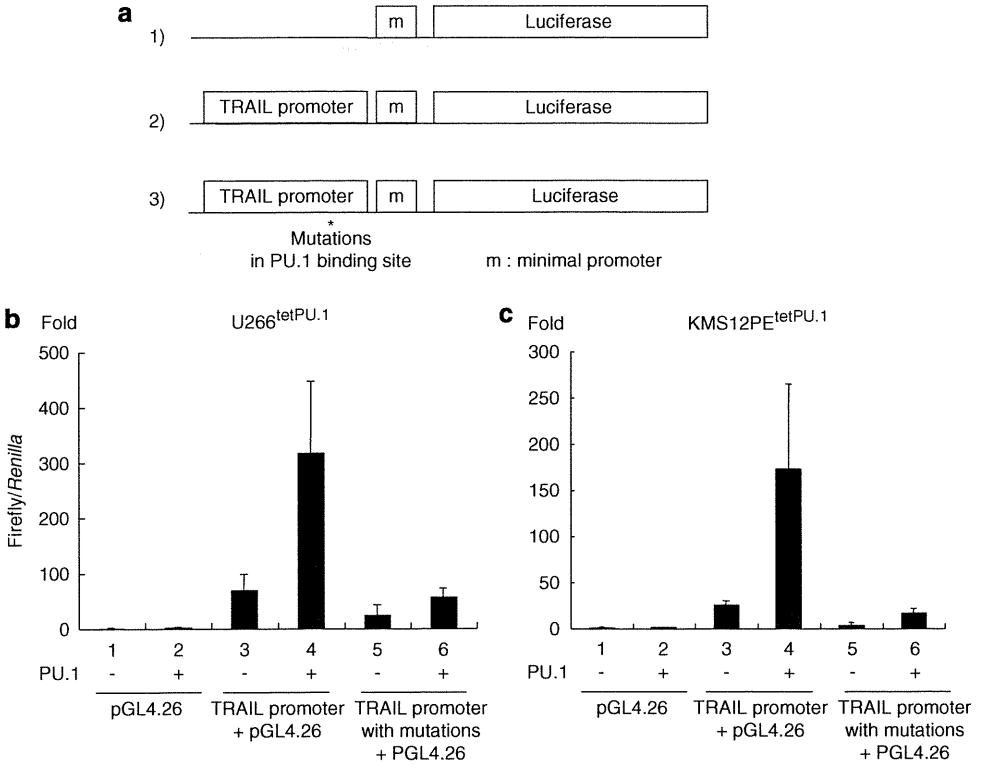

Figure 6 The PU.1 directly transactivates the *TRAIL* promoter in luciferase reporter assays. (**a**) U266$^{tetPU.1}$ and KMS12PE$^{tetPU.1}$ cells were transfected with (1) pGL4.26, (2) pGL4.26 with the *TRAIL* promoter and exon 1 5′-non-coding region, or (3) pGL4.26 with the *TRAIL* promoter and exon 1 5′-non-coding region containing mutations in the PU.1-binding site in the 30-bp 3′-downstream of the transcription start site. pRL-TK was co-transfected to express *Renilla* activity for standardization of the transfection efficiency. (**b, c**) The *TRAIL* promoter activity is dependent on the PU.1-binding site. The Firefly/*Renilla* ratio of U266$^{tetPU.1}$ (**b**) or KMS12PE$^{tetPU.1}$ cells (**c**) before PU.1 induction transfected with pGL4.26 was set as 1 and the transactivation activities are shown as the fold expression. Three independent pools for each plasmid transfection with or without tetracycline were prepared for reporter assays and the mean and the standard deviation for each pool are shown.

CCGGTCACTGAAGCCCTTCCTTC-3′, then subcloned into from *Xho*I site to *Hind*III site of pGL4.26 (*luc2/minP/Hygro*) (Promega). Subsequently, to introduce mutations into the PU.1-binding site in the 30-bp downstream of *TRAIL* transcription start site in the obtained plasmid, self-amplification was performed using primers 5′-CACTGACTATAAAA GAATATCGCAGGAAGGGCTTCAGTGA-3′, and 5′-TCAC TGAAGCCCTTCCTGCGATATTCTTTTATAGTCAGTG-3′ that are located on the almost same region but have opposite directions. In all, 8 μg of these plasmids were transfected with 0.8 μg of pRL-TK plasmid to 8×10^5 of U266$^{tetPU.1}$ or KMS12PE$^{tetPU.1}$ cells with Lipofectamine LTX Reagent (Invitrogen, Carlsbad, CA, USA). Three independent pools for each plasmid were prepared for cultures with or without tetracycline. After 24-h culture, luciferase activity was quantified with Dual-Glo Luciferase Assay System (Promega). Luciferase activity was standardized with dividing by *Renilla* activity.

Conflict of interest

The authors declare no conflict of interest.

Acknowledgements

This work was supported by The Award in Aki's Memory from The International Myeloma Foundation Japan (YO) and grants from the Ministry of Education, Culture, Sports, Science and Technology of Japan.

References

Amaravadi L, Klemsz MJ. (1999). DNA methylation and chromatin structure regulate PU.1 expression. *DNA Cell Biol* **18**: 875–884.

Attal M, Harousseau JL, Facon T, Guilhot F, Doyen C, Fuzibet JG *et al.* (2003). Single versus double autologous stem-cell transplantation for multiple myeloma. *N Engl J Med* **349**: 2495–2502.

Coccia EM, Del Russo N, Stellacci E, Orsatti R, Benedetti E, Marziali G *et al.* (1999). Activation and repression of the 2-5A synthetase and p21 gene promoters by IRF-1 and IRF-2. *Oncogene* **18**: 2129–2137.

de Veer MJ, Sim H, Whisstock JC, Devenish RJ, Ralph SJ. (1998). IFI60/ISG60/IFIT4, a new member of the human IFI54/IFIT2 family of interferon-stimulated genes. *Genomics* **54**: 267–277.

Gazitt Y. (1999). TRAIL is a potent inducer of apoptosis in myeloma cells derived from multiple myeloma patients and is not cytotoxic to hematopoietic stem cells. *Leukemia* **13**: 1817–1824.

Hideshima T, Richardson P, Anderson KC. (2003). Novel therapeutic approaches for multiple myeloma. *Immunol Rev* **194**: 164–176.

Hideshima T, Richardson P, Chauhan D, Palombella VJ, Elliott PJ, Adams J *et al.* (2001). The proteasome inhibitor PS-341 inhibits growth, induces apoptosis, and overcomes drug resistance in human multiple myeloma cells. *Cancer Res* **61**: 3071–3076.

Huang G, Zhang P, Hirai H, Elf S, Yan X, Chen Z *et al.* (2008). PU.1 is a major downstream target of AML1 (RUNX1) in adult mouse hematopoiesis. *Nat Genet* **40**: 51–60.

Iida S, Rao PH, Butler M, Corradini P, Boccadoro M, Klein B *et al.* (1997). Deregulation of MUM1/IRF4 by chromosomal translocation in multiple myeloma. *Nat Genet* **17**: 226–230.

Insinga A, Monestiroli S, Ronzoni S, Gelmetti V, Marchesi F, Viale A *et al.* (2005). Inhibitors of histone deacetylases induce tumor-selective apoptosis through activation of the death receptor pathway. *Nat Med* **11**: 71–76.

Kirshner JR, Karpova AY, Kops M, Howley PM. (2005). Identification of TRAIL as an interferon regulatory factor 3 transcriptional target. *J Virol* **79**: 9320–9324.

Klein U, Casola S, Cattoretti G, Shen Q, Lia M, Mo T *et al.* (2006). Transcription factor IRF4 controls plasma cell differentiation and class-switch recombination. *Nat Immunol* **7**: 773–782.

Klemsz MJ, McKercher SR, Celada A, Van Beveren C, Maki RA. (1990). The macrophage and B cell-specific transcription factor PU.1 is related to the ets oncogene. *Cell* **61**: 113–124.

Li Y, Okuno Y, Zhang P, Radomska HS, Chen H, Iwasaki H *et al.* (2001). Regulation of the PU.1 gene by distal elements. *Blood* **98**: 2958–2965.

Loots GG, Locksley RM, Blankespoor CM, Wang ZE, Miller W, Rubin EM *et al.* (2000). Identification of a coordinate regulator of interleukins 4, 13, and 5 by cross-species sequence comparisons [see comments]. *Science* **288**: 136–140.

Mariani SM, Matiba B, Armandola EA, Krammer PH. (1997). Interleukin 1 beta-converting enzyme related proteases/caspases are involved in TRAIL-induced apoptosis of myeloma and leukemia cells. *J Cell Biol* **137**: 221–229.

McKercher SR, Torbett BE, Anderson KL, Henkel GW, Vestal DJ, Baribault H *et al.* (1996). Targeted disruption of the PU.1 gene results in multiple hematopoietic abnormalities. *Embo J* **15**: 5647–5658.

Mitsiades CS, Treon SP, Mitsiades N, Shima Y, Richardson P, Schlossman R *et al.* (2001). TRAIL/Apo2 L ligand selectively induces apoptosis and overcomes drug resistance in multiple myeloma: therapeutic applications. *Blood* **98**: 795–804.

Mitsiades N, Mitsiades CS, Poulaki V, Anderson KC, Treon SP. (2002). Intracellular regulation of tumor necrosis factor-related apoptosis-inducing ligand-induced apoptosis in human multiple myeloma cells. *Blood* **99**: 2162–2171.

Moreau-Gachelin F, Tavitian A, Tambourin P. (1988). Spi-1 is a putative oncogene in virally induced murine erythroleukaemias. *Nature* **331**: 277–280.

Nebbioso A, Clarke N, Voltz E, Germain E, Ambrosino C, Bontempo P *et al.* (2005). Tumor-selective action of HDAC inhibitors involves TRAIL induction in acute myeloid leukemia cells. *Nat Med* **11**: 77–84.

Okuno Y, Huang G, Rosenbauer F, Evans EK, Radomska HS, Iwasaki H *et al.* (2005). Potential autoregulation of transcription factor PU.1 by an upstream regulatory element. *Mol Cell Biol* **25**: 2832–2845.

Okuno Y, Huettner CS, Radomska HS, Petkova V, Iwasaki H, Akashi K *et al.* (2002a). Distal elements are critical for human CD34 expression *in vivo*. *Blood* **100**: 4420–4426.

Okuno Y, Iwasaki H, Huettner CS, Radomska HS, Gonzalez DA, Tenen DG *et al.* (2002b). Differential regulation of the human and murine CD34 genes in hematopoietic stem cells. *Proc Natl Acad Sci USA* **99**: 6246–6251.

Pahl HL, Scheibe RJ, Zhang DE, Chen HM, Galson DL, Maki RA *et al.* (1993). The proto-oncogene PU.1 regulates expression of the myeloid-specific CD11b promoter. *J Biol Chem* **268**: 5014–5020.

Radomska HS, Gonzalez DA, Okuno Y, Iwasaki H, Nagy A, Akashi K *et al.* (2002). Transgenic targeting with regulatory elements of the human CD34 gene. *Blood* **100**: 4410–4419.

Rosenbauer F, Owens BM, Yu L, Tumang JR, Steidl U, Kutok JL *et al.* (2006). Lymphoid cell growth and transformation are suppressed by a key regulatory element of the gene encoding PU.1. *Nat Genet* **38**: 27–37.

Rosenbauer F, Wagner K, Kutok JL, Iwasaki H, Le Beau MM, Okuno Y *et al.* (2004). Acute myeloid leukemia induced by graded reduction of a lineage-specific transcription factor, PU.1. *Nat Genet* **36**: 624–630.

Shaffer AL, Emre NC, Lamy L, Ngo VN, Wright G, Xiao W *et al.* (2008). IRF4 addiction in multiple myeloma. *Nature* **454**: 226–231.

Singhal S, Mehta J, Desikan R, Ayers D, Roberson P, Eddlemon P *et al.* (1999). Antitumor activity of thalidomide in refractory multiple myeloma. *N Engl J Med* **341**: 1565–1571.

Tatetsu H, Ueno S, Hata H, Yamada Y, Takeya M, Mitsuya H *et al.* (2007). Down-regulation of PU.1 by methylation of distal regulatory elements and the promoter is required for myeloma cell growth. *Cancer Res* **67**: 5328–5336.

Tenen DG. (2003). Disruption of differentiation in human cancer: AML shows the way. *Nat Rev Cancer* **3**: 89–101.

Yu W, Misulovin Z, Suh H, Hardy RR, Jankovic M, Yannoutsos N *et al.* (1999). Coordinate regulation of RAG1 and RAG2 by cell type-specific DNA elements 5′ of RAG2. *Science* **285**: 1080–1084.

Supplementary Information accompanies the paper on the Oncogene website (http://www.nature.com/onc)

Int J Hematol
DOI 10.1007/s12185-009-0314-5

ORIGINAL ARTICLE

Phase II and pharmacokinetic study of thalidomide in Japanese patients with relapsed/refractory multiple myeloma

Hirokazu Murakami · Kazuyuki Shimizu · Morio Sawamura · Kenshi Suzuki · Isamu Sugiura · Hiroshi Kosugi · Chihiro Shimazaki · Masafumi Taniwaki · Masahiro Abe · Toshiyuki Takagi

Received: 9 February 2009 / Revised: 25 March 2009 / Accepted: 31 March 2009

Abstract To obtain approval from the Ministry of Health, Labor and Welfare of Japan, a phase II study was conducted to assess the pharmacokinetics and pharmacodynamics of thalidomide along with its efficacy and safety in Japanese patients with multiple myeloma. Between 2005 and 2006, 42 patients were enrolled, and 37 patients met eligibility criteria. Of the 37 patients, 3 were excluded from efficacy analysis because of short duration of thalidomide administration (<4 weeks). The overall response rate was 35.3% (12/34), including partial response of 14.7% (5/34) and minimal response of 20.6% (7/34). The adverse events observed in high frequency (>40%) were leukopenia, neutropenia, drowsiness, dry mouth, and constipation. Grade 3 neutropenia was observed in nine cases. Peripheral neuropathy and eruption were observed in about one-quarter of the patients. Deep vein thrombosis was not observed. At a single oral dose of thalidomide (100 mg), the C_{max} was 1.68 ± 0.41 μg/ml, T_{max} was 4.54 ± 1.71 h, $T_{1/2}$ was 4.86 ± 0.44 h, and AUC was 15.87 ± 3.05 μg h/ml. Low-dose thalidomide was an effective and tolerable treatment for Japanese patients with relapsed/refractory myeloma. Leukopenia and neutropenia were the most serious adverse events. The pharmacokinetics was similar to those observed in Caucasian patients.

Keywords Myeloma · Thalidomide · Adverse event · Pharmacokinetics

H. Murakami (✉)
Faculty of Medicine, School of Health Sciences,
Gunma University, Showa-machi 3-39-15,
Maebashi, Gunma 371-8511, Japan
e-mail: hmura@health.gunma-u.ac.jp

K. Shimizu
Department of Internal Medicine, Nagoya City Midori General Hospital, Nagoya, Japan

M. Sawamura
Department of Internal Medicine, Nishi-Gunma Hospital, Shibukawa, Japan

K. Suzuki
Department of Hematology, Japanese Red Cross Medical Center Hospital, Tokyo, Japan

I. Sugiura
Department of Hematology and Oncology,
Toyohashi Municipal Hospital, Toyohashi, Japan

H. Kosugi
Department of Hematology, Ogaki Municipal Hospital,
Ogaki, Japan

C. Shimazaki · M. Taniwaki
Department of Molecular Hematology and Oncology,
Graduate School of Medical Science, Kyoto Prefectural University, Kyoto, Japan

M. Abe
Department of Medicine and Bioregularoty Sciences,
Tokushima University, Tokushima, Japan

T. Takagi
Department of Hematology and Oncology,
Kimitsu Chuou Hospital, Kisarazu, Japan

Published online: 28 April 2009

1 Introduction

Multiple myeloma is a clonal disorder of plasma cells that accounts for 10% of hematological malignancies. The median overall survival has been improved by high-dose chemotherapy with autologous stem cell transplantation (ASCT) [1], as well as by the emergence of novel therapies, which improved post-relapse survival and overall survival as well [2].

One of the novel agents, thalidomide was introduced to the market in the 1950s as a sedative. However, in 1961, Lenz reported a close relationship between the administration of thalidomide to pregnant women and the development of a deformity in their babies [3]. In Japan the withdrawal of thalidomide was incomplete and late, and over 1,000 babies suffered on account of thalidomide. After that thalidomide disappeared from the Japanese drug market. In 1994, D'Amato et al. [4] showed that thalidomide inhibited angiogenesis in rabbits and suggested thalidomide as a therapeutic agent for diseases that involve angiogenesis, particularly those of malignant tumors. Furthermore, in 1994, Vacca et al. [5] reported that the bone marrow of patients with myeloma was rich in microvessels and that there was a positive relationship between the disease activity of multiple myeloma and the density of bone marrow microvasculatures. Based on these data, a clinical trial with thalidomide was initiated in many countries to investigate the potential of thalidomide as a new therapeutic agent for patients with relapsed/refractory myeloma. Singhal et al. [6] reported the efficacy of thalidomide as single agent in patients with refractory myeloma. In their study, thalidomide was administered nightly at a dose of 200 mg/day. The dose was increased by 200 mg every 2 weeks up to 800 mg/day. An overall response rate of 32% and a 1-year survival rate of 58% were reported involving 84 patients with refractory myeloma. In addition, they showed that the response rate and survival were improved by escalating the doses of thalidomide. Most adverse events were grade 1 and 2. Constipation, weakness and fatigue, and somnolence occurred in one-third or more of the patients. In recent years, low-dose thalidomide therapy has been tested in many countries whether it reduces the risk of such adverse events without jeopardizing its efficacy. According to these reports, thalidomide may be effective in Japanese patients with relapsed/refractory multiple myeloma like Caucasian patients.

The present phase II study was designed to assess the efficacy and toxicity of the thalidomide treatment in Japanese patients with relapsed/refractory myeloma. The primary endpoint of this study was response rate. The secondary endpoint was toxicity.

2 Patients and methods

Only patients with the diagnosis of multiple myeloma according to the South-West Oncology Group criteria, those who have relapsed after high-dose chemotherapy with ASCT, those who have progressed after the maximum of three previous standard chemotherapies, and those who were >20 years of age and Eastern Cooperative Oncology Group (ECOG) performance status <3 were eligible for the study. The following patients were excluded from the study: pregnant women and female patients with the possibility of conception; patients with non-secretory myeloma, plasma cell leukemia, or plasmacytoma; those previously treated with thalidomide; those with abnormal renal function (serum creatinine >3.0 mg/dl); those with low white blood cell count ($<2 \times 10^6$/ml); those with abnormal liver function (aspartate aminotransferase and alanine aminotransferase levels >3 times the upper limit of institutional normal range); those with a past medical history of deep vein thrombosis; and those with high serum FDP. This study was approved by the institutional review board of each participating hospital. All patients gave a written informed consent and the study was conducted in accordance with the Good Clinical Practice for Trials of Drugs and the Declaration of Helsinki.

With type I error of 0.05, 24 patients were required for the study to have 80% power to reject the null hypothesis of response rate of 7% against the alternative hypothesis of response rate 42%.

Thalidomide, supplied by Fujimoto Pharmaceutical Corporation (Osaka, Japan), was administered orally at a dosage of 100 mg/day before sleep for the first 4 weeks with an increase in dosage to 200 mg/day between weeks 5 and 8, an increase to 300 mg/day between weeks 9 and 12, and finally to the maximum dose of 400 mg/day from the week 13, only if a patient did not experience non-hematological toxicities greater than grade 2 and/or hematological toxicities greater than grade 3 according to the National Cancer Institute Common Toxicity Criteria (NCI-CTC), version 2.0 criteria. If minimal, partial, or complete response was obtained with the treatment, thalidomide was maintained at the final dose. Anti-thrombotic prophylaxis was not instituted in this study.

Patients were monitored for response by quantitating serum and/or urine paraprotein with electrophoresis every 2 weeks and at the time of protocol discontinuation. Response was determined according to the EBMT criteria: complete response, disappearance of paraprotein at least 4 weeks apart; partial response, ≥50% decrease from the baseline paraprotein levels at least 4 weeks apart; minimal response, ≥25% decrease; no change, <25% decrease; progressive disease, ≥25% increase from the baseline

paraprotein levels. Adverse events were assessed and graded according to the NCI-CTC, version 2.0 criteria.

2.1 Pharmacokinetic analysis

Plasma thalidomide concentration was measured as the phase I study. Blood samples were collected before the administration of 100 mg thalidomide and at 1, 2, 3, 4, 6, 8, 12, and 24 h on the first day. Thalidomide concentration in the plasma was determined with the use of high-performance liquid chromatography (HPLC), by a modified version of the methods of Figgs et al. [7] and Simmons et al. [8].

3 Results

3.1 Patients and dose escalation

The study was conducted between July 2005 and June 2006, and comprised 42 patients. Of these, 37 patients met the eligibility criteria; another 4 patients were not treated with thalidomide because of disease progression and the remaining 1 patient was excluded from the study protocol because of high serum FDP. The characteristics of the 37 eligible patients are shown in Table 1. The male/female ratio was 0.6 (14/23) and the median age was 63 years (range 42–81 years). The immunoglobulin subtypes were IgG, 22 patients; IgA, 12 patients; and light chain only, 3 patients. The median time to treatment start since diagnosis was 4.1 years (range 0.2–17 years). Performance statuses were 0, 21 patients; 1, 15 patients; and 2, 1 patient. Sixteen patients had recurrence after ASCT and the remaining 21 patients were refractory to or relapsed from prior conventional chemotherapies.

Table 1 Patients' characteristics

No. of patients	37
Male/female	14/23
Age	
Median	63
Range	42–81
Time since diagnosis	
Median	4.1
Range	0.2–17
PS 0/1/2	21/15/1
Ig subtype (IgG/IgA/BJP)	22/12/3
Prior therapy	
Chemotherapy	21
ASCT	16

The mean dose of thalidomide was 100 mg/day at the 4th week, 177.8 mg/day at the 6th week, 166.7 mg/day at the 8th week, and 200 mg/day throughout weeks 10 to 16 (Fig. 1).

3.2 Efficacy (Table 2)

Of the 37 patients, 3 with short duration of thalidomide administration ($\leq$4 weeks) were excluded from the efficacy analysis because Singhal et al. [6] reported that the median time to a reduction in the serum or urine paraprotein level of at least 25, 50, 75, and 90% were 1, 2, 4, and 4 months, respectively. Of the remaining 34 patients, no patient achieved a complete response, 5 (14.7%) achieved a partial response and 7 (20.6%) achieved a minimal response. The overall response rate of the present study (partial response + minimal response) was 35.3%. In another 12 patients (35.3%), there was no change in the M-protein levels; in another 6 patients, progressive disease was observed; in the remaining 4 patients, the effect of treatment was not evaluated because the observation period of response was shorter than 4 weeks. The response rate at a dose of 100 mg/day was 45.0% that at 200 mg/day was 28.6%, that at 300 mg/day was 50.0%, and that at 400 mg/day was 0%. The overall response rate decreased as patient age increased (40–49 years, 75.0%; 50–59 years, 40.0%; 60–69 years, 33.3%; and $\geq$70 years, 18.2%). The progression-free survival at 2 year was 44.0% (Fig. 2).

3.3 Adverse events

The safety analysis data set consisted of 37 patients who actually received thalidomide therapy. Adverse events observed in $\geq$15% of patients are shown in Table 3. Adverse events observed at higher frequency (>40%) were leukopenia, neutropenia, drowsiness, dry mouth, and constipation. Non-hematological adverse events over grade 2 were observed in only two cases; those events were

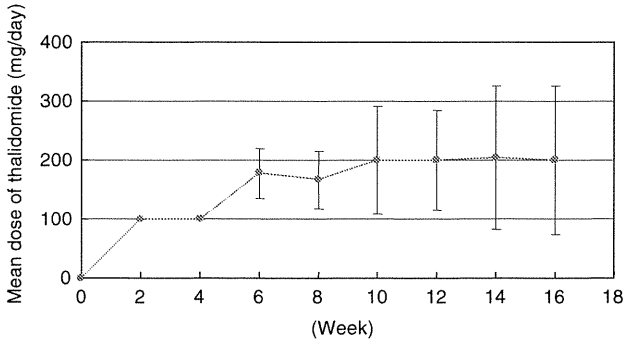

Fig. 1 The mean dose of thalidomide was 100 mg/day at week 4, 177.8 mg/day at week 6, 166.7 mg/day at week 8, and 200 mg/day between week 10 and week 16

Table 2 Response to thalidomide treatment

	Complete response	Partial response	Minimal response	No change	Progressive disease	Not evaluated	Overall response
100 mg/day (20 cases)	0 (0%)	5 (25.0%)	4 (20.0%)	(25.0%)	4 (20.0%)	2 (10.0%)	9 (45.0%)
200 mg/day (7 cases)	0 (0%)	0 (0%)	2 (28.6%)	2 (28.6%)	1 (14.3%)	2 (28.6%)	2 (28.6%)
300 mg/day (2 cases)	0 (0%)	0 (0%)	1 (50%)	0 (0%)	1 (50%)	0 (0%)	1 (50%)
400 mg/day (5 cases)	0 (0%)	0 (0%)	0 (0%)	5 (100%)	0 (0%)	0 (0%)	0 (0%)
All dosages (34 cases)	0 (0%)	5 (14.7%)	7 (20.6%)	12 (35.3%)	6 (17.6%)	4 (11.8%)	12 (35.3%)

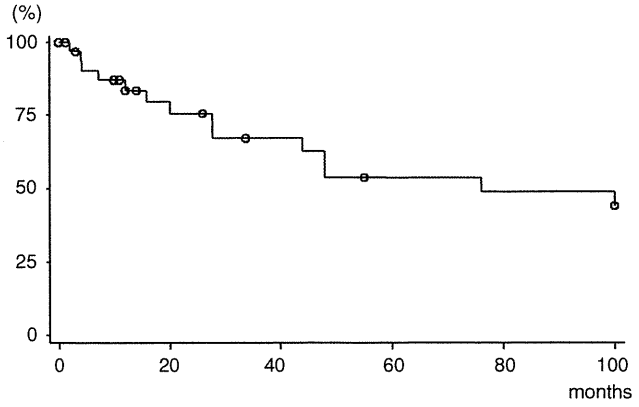

Fig. 2 The progression-free survival at 2 years was 44.0%

ischemic heart disease and perforation of the intestine. Of the hematological adverse events greater than grade 2, leukopenia was seen in five cases, neutropenia in nine cases, and lymphopenia in three cases. Therapy-related mortality was not observed in this study.

3.4 Pharmacokinetics

The mean plasma thalidomide concentration–time profile at 0, 1, 2, 3, 4, 6, 8, 12, and 24 h in 12 patients who received 100 mg of thalidomide is shown in Fig. 3. Pharmacokinetic parameters obtained using non-compartmental analysis are shown in Table 4. The C_{max} was 1.68 ± 0.41 μg/ml, T_{max} was 4.54 ± 1.71 h, $T_{1/2}$ was 4.86 ± 0.44 h, and AUC was 15.87 ± 3.05 μg h/ml, respectively.

4 Discussion

The response rate of thalidomide used as a single agent in patients with relapsed/refractory multiple myeloma has been reported as 30–40%. Barlogie et al. [9] analyzed the efficacy according to various doses of thalidomide in a phase-II study. They found that patients who were administered more than 42 g of a cumulative dose of thalidomide in a 3-month period had a greater M-protein reduction rate and a longer survival than others who were administered smaller cumulative doses of thalidomide, in high-risk patients as well as in low-risk patients. On the other hand, Durie et al. [10] reported that with a thalidomide dose of only 200 mg/day, an overall response ≥ minimal response was obtained in 44% and the survival rate at 2 years was 22%. Johnston et al. [11] also reported that partial response was obtained in 42% of patients with resistant/refractory myeloma by low-dose thalidomide therapy (median 175 mg/day) with a lower incidence of adverse events. In our study, the overall response rate was 35.5%, comparable to those of other reports. The median dose of thalidomide was about 200 mg/day after 6 months. According to these data, low-dose thalidomide is considered effective in Japanese patients as well.

Regarding hematological adverse events, neutropenia was observed in about half of the patients and neutropenia over grade 2 occurred in 24.3%. This adverse event has been rarely reported in Caucasian individuals, but was reported in a significantly higher incidence in Japanese individuals [12, 13]. Thus, the risk of neutropenia has to be kept in mind in Japanese patients with multiple myeloma treated with thalidomide. In non-hematological adverse events, drowsiness was seen in 54.1%, dry mouth in 43.2%, and constipation in 62.2%. All of these adverse events were less than grade 3 in severity. Peripheral neuropathy and eruption were observed in about one-quarter of the patients and the incidence was comparable to that observed in the USA and Europe [14]. Deep vein thrombosis was not observed in this study, unlike the relatively higher incidence reported from USA and Europe [14, 15]. The reason for the contradictory finding in the incidence of deep vein thrombosis in Japanese patients is unclear, but aside from the small number of patients studied, ethnic differences may have contributed. In addition, the lower dose of thalidomide administered may have resulted in this. The incidence of deep vein thrombosis has been reported to increase when dexamethasone and/or anticancer drugs such as doxorubicin were combined with thalidomide [14]; however, this was not the case in this study.

Noormohamed et al. [16] reported that C_{max} was 1.15 μg/ml and AUC was 9.8 μg h/ml when thalidomide was administered at a single dose of 100 mg. In our study,

Table 3 All adverse events occurring in at least 15% of patients ($n = 37$)

Adverse event	NCI-CTC grade				Total
	1	2	3	4	
Hematological					
Leukopenia	4 (10.8%)	6 (16.2%)	5 (13.5%)	0	15 (40.5%)
Neutropenia	3 (8.1%)	5 (13.5%)	9 (24.3%)	0	17 (49.5%)
Lymphopenia	2 (5.4%)	2 (5.4%)	3 (8.1%)	0	7 (18.9%)
Thrombocytopenia	6 (16.2%)	1 (2.7%)	0	0	7 (18.9%)
Non-hematological					
Eruption	8 (21.6%)	2 (5.4%)	0	0	10 (27.0%)
Trembling	10 (27.0%)	0	0	0	10 (27.0%)
Dizziness	7 (18.9%)	0	0	0	7 (18.9%)
Numbness of extremities	8 (21.6%)	1 (2.7%)	0	0	9 (24.3%)
Numbness of lip	8 (21.6%)	0	0	0	8 (21.6%)
Gustatory disturbance	8 (21.6%)	0	0	0	8 (21.6%)
Drowsiness	20 (54.1%)	0	0	0	20 (54.1%)
Dry mouth	16 (43.2%)	0	0	0	16 (43.2%)
Constipation	22 (59.5%)	1 (2.7%)	0	0	23 (62.2%)
Nausea	7 (18.9%)	0	0	0	7 (18.9%)
Abdominal distention	6 (16.2%)	0	0	0	6 (16.2%)
Fatigue	10 (27.0%)	1 (2.7%)	0	0	11 (29.7%)
Edema	6 (16.2%)	0	0	0	6 (16.2%)

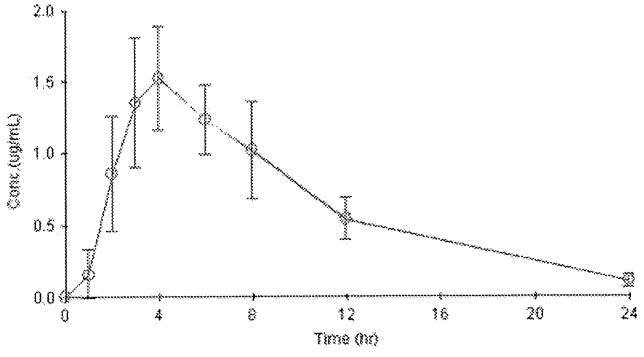

Fig. 3 The mean plasma thalidomide concentration–time profile at 0, 1, 2, 3, 4, 6, 8, 12, and 24 h in 12 patients who received 100 mg of thalidomide

Table 4 Pharmacokinetic parameter

Parameter		
C_{max}	1.68 ± 0.41	μg/mL
T_{max}	4.54 ± 1.71	h
$T_{1/2}$	4.86 ± 0.44	h
AUC	15.87 ± 3.05	μg h/ml
Cl	6507 ± 1172	ml/h
Vd	45336 ± 7454	ml
kel	0.144 ± 0.012	1/h
MRT	9.06 ± 1.07	h
AUMC	145.08 ± 40.20	h × h × μg/ml

C_{max} maximum drug concentration, T_{max} maximum drug concentration time, $T_{1/2}$ half-life period, *AUC* area under the concentration–time curve from 0 to infinity, *Cl* clearance, *Vd* distribution volume, *kel* k (elimination rate constant), *MRT* mean resident time, *AUMC* area under the moment curve

C_{max} was 1.68 μg/ml and AUC was 15.9 μg h/ml, both of which were higher than the data of Noormohamed et al. The Japanese patients had lower body weight; the C_{max} became 1.28 μg/ml and AUC 12.2 μg h/ml when adjusted for body weight, both of the adjusted data turned out to be similar to Noormohamed's data. According to these data, thalidomide was considered to be well absorbed when administered orally in Japanese patients.

5 Conclusions

Low-dose thalidomide treatment was effective and tolerable in Japanese patients with relapsed/refractory multiple myeloma. The pharmacokinetics was similar to those observed in Caucasian patients. In addition to the authors, the following investigators participated in this study.

Sadao Ishida, Toshiaki Hayashi (Sapporo Medical University), Norifumi Tsukamoto, Hiroshi Handa, Takayuki Saitoh, Arito Yamane (Gunma University), Akihiro Ishii (Chiba Cancer Center), Shinichiro Okamoto, Yutaka Hattori (Keio University), Akiyoshi Miwa, Mutsumi Matsumaru, Kimito Kawahata (International Medical Center of Japan, Toyama Hospital), Masatsugu

Ohta (Tokyou Metropolitan Geriatric Medical Center), Masaaki Yuge (Ogaki Municipal Hospital), Shinsuke Iida, Shigeru Kusumoto (Nagoya City University), Yutaka Kobayashi, Kenichi Nomura, Kazuho Shimura (Kyoto Prefectural University), Takayuki Ishikawa, Norimitsu Kadowaki (Kyoto University), Hitoshi Nakagawa, Toshiki Iwai (Red Cross Kyoto Daiichi Hospital), Yuzuru Kanakura, Jun Ishikawa, Masao Mizuki (Osaka University), Takashi Sonoki (Wakayama Medical University), Kazuki Sunami (Okayama Medical Center), Hideki Asaoku (Hiroshima Red Cross Hospital & Atomic-bomb Survivors Hospital), Akira Sakai (Hiroshima University), Hiroatsu Ago, Toshio Wakayama (Shimane Prefectural Central Hospital), Shuji Ozaki (Tokushima University), Hiroyuki Hata (Kumamoto University).

References

1. Attal M, Harousseau J-L, Facon T, Guilhot F, Doyen C, Fuzibet J-G, et al. Single versus double autologous stem-cell transplantation for multiple myeloma. N Engl J Med. 2003;349:2495–502.
2. Kumar SK, Rajkumar SV, Dispenzieri A, Lacy MQ, Hayman SR, Buadi FK, et al. Improved survival in multiple myeloma and the impact of novel therapies. Blood. 2008;111:2516–20. doi: 10.1182/blood-2007-10-116129.
3. Lenz W. Thalidomide embryopathy in Germany, 1959–1961. Prog Clin Biol Res. 1985;163C:77–83.
4. D'Amato RJ, Loughnan MS, Flynn E, Folkman J. Thalidomide is an inhibitor of angiogenesis. Proc Natl Acad Sci USA. 1994;91:4082–5.
5. Vacca A, Ribatti D, Roncali L, Ranieri G, Serio G, Silvestris F, et al. Bone marrow angiogenesis and progression in multiple myeloma. Br J Haematol. 1994;87:503–8. doi:10.1111/j.1365-2141.1994.tb08304.x.
6. Singha S, Mehta J, Desikan R, Ayers D, Roberson P, Eddlemon P, et al. Antitumor activity of thalidomide in refractory multiple myeloma. N Engl H Med. 1999;341:1565–71.
7. Figg WD, Raje S, Bauer KS, Tompkins A, Venzon D, Bergan R, et al. Pharmacokinetics of thalidomide in an elderly prostate cancer population. J Pharm Sci. 1999;88:121–5.
8. Simmons BR, Lush RM, Figg WD. A reversed-phase high performance liquid chromatography method using solid phase extraction to quantitate thalidomide in human serum. Anal Chim Acta. 1997;339:91–7. doi:10.1016/S0003-2670(96)00494-1.
9. Barlogie B, Zangari M, Spencer T, Fassas A, Anaissie E, Badros A, et al. Thalidomide in the management of multiple myeloma. Semin Haematol. 2001;38:250–9.
10. Durie BGM. Low-dose thalidomide in myeloma: efficacy and biologic significance. Semin Oncol. 2002;29 Suppl 17:34–8.
11. Johnston RE, Abdalla SH. Thalidomide in low doses in effective for the treatment of resistant or relapsed multiple myeloma and for plasma cell leukaemia. Leukemia Lymphoma. 2002;43:351–4.
12. Murakami H, Handa H, Abe M, Iida S, Ishii A, Ishikawa T, et al. Low-dose thalidomide plus low-dose dexamethasone therapy in patients with refractory multiple myeloma. Eur J Haematol. 2007;79:234–9.
13. Hattori Y, Okamoto S, Shimada N, Kakimoto T, Morita K, Tanigawara Y, et al. Single-institute phase 2 study of thalidomide treatment for refractory or relapsed multiple myeloma: prognostic factors and unique toxicity profile. Cancer Sci. 2008;99:1243–50.
14. Matthews SJ, McCoy C. Thalidomide: a review of approved and investigational uses. Clin Therap. 2003;25:356–61.
15. Rajkumar SV, Rosiñol L, Hussein M, Catalano J, Jedrzejczak W, Lucy L, et al. Multicenter, randomized, double-blind, placebo-controlled study of thalidomide plus dexamethasone compared with dexamethasone as initial therapy for newly diagnosed multiple myeloma. J Clin Oncol. 2008;26:2171–7.
16. Noormohamed FH, Youle MS, Higgs CJ, Kook KA, Hawkins DA, Lant AF, et al. Pharmacokinetics and hemodynamic effects of single oral doses of thalidomide in asymptomatic human immunodeficiency virus-infected subjects. AIDS Res Human Retroviruses. 1999;15:1047–52.

Leukemia (2010), 1–8

www.nature.com/leu

ORIGINAL ARTICLE

Galectin-9 exhibits anti-myeloma activity through JNK and p38 MAP kinase pathways

T Kobayashi[1], J Kuroda[1], E Ashihara[2], S Oomizu[3], Y Terui[4], A Taniyama[4], S Adachi[5], T Takagi[5], M Yamamoto[1], N Sasaki[1], S Horiike[1], K Hatake[4], A Yamauchi[6], M Hirashima[3] and M Taniwaki[1]

[1]Division of Hematology and Oncology, Department of Medicine, Kyoto Prefectural University of Medicine, Kyoto, Japan; [2]Department of Transfusion Medicine and Cell Therapy, Kyoto University Hospital, Kyoto, Japan; [3]Department of Immunology and Immunopathology, Faculty of Medicine, Kagawa University, Kagawa, Japan; [4]Division of Clinical Chemotherapy, Cancer Chemotherapy Center, Japanese Foundation for Cancer Research, Tokyo, Japan; [5]Department of Gastroenterology, Kyoto Prefectural University of Medicine, Kyoto, Japan and [6]Department of Cell Regulation, Faculty of Medicine, Kagawa University, Kagawa, Japan

Galectins constitute a family of lectins that specifically exhibit the affinity for β-galactosides and modulate various biological events. Galectin-9 is a tandem-repeat type galectin with two carbohydrate recognition domains and has recently been shown to have an anti-proliferative effect on cancer cells. We investigated the effect of recombinant protease-resistant galectin-9 (hGal9) on multiple myeloma (MM). *In vitro*, hGal9 inhibited the cell proliferation of five myeloma cell lines examined, including a bortezomib-resistant subcell line, with IC_{50} between 75.1 and 280.0 nM, and this effect was mediated by the induction of apoptosis with the activation of caspase-8, -9, and -3. hGal9-activated Jun NH_2-terminal kinase (JNK) and p38 MAPK signaling pathways followed by H2AX phosphorylation. Importantly, the inhibition of either JNK or p38 MAPK partly inhibited the anti-proliferative effect of hGal9, indicating the crucial role of these pathways in the anti-MM effect of hGal9. hGal9 also induced cell death in patient-derived myeloma cells, some with poor-risk factors, such as chromosomal deletion of 13q or translocation t(4;14)(p16;q32). Finally, hGal9 potently inhibited the growth of human myeloma cells xenografted in nude mice. These suggest that hGal9 is a new therapeutic target for MM that may overcome resistance to conventional chemotherapy.
Leukemia advance online publication, 4 March 2010; doi:10.1038/leu.2010.25
Keywords: galectin-9; H2AX; JNK; multiple myeloma; p38

Introduction

Galectins constitute a family of animal lectins that show affinity for β-galactosides and share conserved amino-acid sequences in their carbohydrate recognition domains.[1,2] Fourteen mammalian galectins, galectin-1 to -14, are classified into three subtypes according to their structure, that is, prototype, chimera, and tandem-repeat type. The tandem-repeat type galectins with two carbohydrate recognition domains that recognize different sugar binding target molecules are capable of cross-linking with a wider variety of glycoconjugates than other subtypes.[3] Galectin-9 is a tandem-repeat type galectin, and has been shown to be involved in a variety of cellular functions, such as cell adhesion, proliferation, and apoptosis.[4–10] Moreover, recent studies have indentified anti-cancer properties of galectin-9 against several cancers.[11–15] In this study, we show the anti-multiple myeloma (MM) activity of a recombinant mutant form of human galectin-9 (hGal9) through the activation of c-Jun NH_2-terminal kinase (JNK) and p38 mitogen-activated protein kinase (MAPK) signaling pathways, those share crucial roles in the survival and death of myeloma cells.[16]

Correspondence: Dr J Kuroda, Division of Hematology and Oncology, Department of Medicine, Kyoto Prefectural University of Medicine, 465 Kajii-cho, Kamigyo-ku, Kyoto 602-8566, Japan.
E-mail: junkuro@koto.kpu-m.ac.jp
Received 5 September 2009; revised 30 December 2009; accepted 21 January 2010

Materials and methods

Cell lines and reagents

MM cell lines IM9, KMS-12-BM, AMO-1, NCI-H929, and RPMI8226 were maintained as described earlier.[17] The IM9 subline with lower sensitivity to bortezomib (Bor) (IM9-Bor), established by Dr Terui Y, was maintained with 20 nM Bor. The recombinant hGal9, which is highly stable against proteolysis, was synthesized by Galpharma (Kagawa, Japan).[18] JNK-inhibitor VIII, SB203580, an inhibitor for p38 MAPK, Z-VAD-FMK, Z-IETD-FMK, and Z-LEHD-FMK were purchased from Calbiochem (San Diego, CA, USA) and lactose was purchased from Sigma (St Louis, MO, USA).

Primary human myeloma samples

Studies with patient samples were approved by the Ethics Board of our institute. Bone marrow (BM) mononuclear cells were labeled with anti-CD138 MicroBeads and were positively isolated with the MiniMACS separator (Miltenyi Biotec KK, Tokyo, Japan). More than 98% of the cells isolated were morphologically confirmed as plasma cells after Wright-Giemsa staining, and were cultured with 20 ng/ml interleukin-6.

Cell surface binding affinity of hGal9

Cells were incubated with biotinylated human Gal-9 NC (hGal9NC) (Galpharma) in 2.0% FCS-containing PBS buffer supplemented with 2 μg/ml Streptavidin-FITC. For negative control, cells were incubated only with Streptavidin-FITC. Cells were washed twice and subjected to flow cytometric analyses.

Assays for growth inhibition and apoptosis

Growth-inhibitory effect of hGal9 was analyzed with a modified MTT assay using Cell Counting Kit-8 (Dojindo, Japan) or by direct counting of cell number. Data represent the results of means ± standard errors of three independent experiments. To determine apoptosis, cells were counterstained with propidium iodide and Annexin V-FITC. Mitochondrial outer membrane

potential (MOMP) was assayed using MitoScreen (JC-1) Kit (Beckton Dickinson, San Diego, CA, USA).

Microarray analysis

IM9 and KMS-12-BM were treated with or without 100 nM hGal9 for 6 h, and total RNA was isolated. Gene expression was analyzed with Affymetrix Gene Chip arrays and GeneChip Scanner 3000 (Affymetrix, Santa Clara, CA, USA), and array data analysis was carried out with Affymetrix GeneChip operating software version 1.0. Genes showing at least a 2.0-fold difference in expression levels between control and hGal9-treated cells were considered to be modulated by hGal9. Data were also analyzed with the Ingenuity pathway analysis software (Ingenuity Systems, Mountain View, CA, USA).

Quantitative RT-PCR (RQ-PCR)

RQ-PCR was performed as was described earlier.[19] Primers used were as follows: *c-jun* 5′-tgactgcaaagatggaaacg-3′ and 5′-ccgttgctggactggattat-3′, *jun-D* 5′-ctcaaggacgagccacagac-3′ and 5′-tggctgaggactttctgctt-3′.

Western blotting

Western blotting was performed as was described elsewhere.[19,20] Primary antibodies (Abs) used were those against JNK, p38 MAPK, phosphorylated p38 MAPK, caspase-3, caspase-8, caspase-9 (Cell Signaling Technologies, Beverly, MA, USA), H2AX, phosphorylated H2AX (Upstate Biotechnology, Inc., Lake Placid, NY, USA), phosphorylated JNK, c-Jun, Jun-D (Santa Cruz Biotechnology, Santa Cruz, CA, USA), and β-tubulin (Sigma).

In vivo anti-myeloma activity of hGal9

Animal studies were performed according to the guidelines of the institutional review board. In all, 5×10^6 IM9 cells were subcutaneously injected into the right hind flank of ten 6-week-old nude mice, which had been whole-body irradiated with 2 Gy 24 h before tumor implantation. Tumor volume was calculated with the formula $V = 0.5a \times b^2$, where a is the long and b is the short diameter of the tumor. Mice were randomized into two groups, five mice for hGal9 treated and five mice for control, when the mean tumor volume reached 400 mm^3. In all, 100 μg/body/day of hGal9 or PBS was administered to the respective groups for 14 consecutive days through intrapenitoneal injection. Volume of tumors of hGal9-treated mice was compared with that of vehicle-treated controls with the Mann–Whitney *U*-test. A *P*-value of <0.05 was considered statistically significant.

Results

Anti-myeloma effect of hGal9 through induction of apoptosis in vitro

hGal9 displays a growth-inhibitory effect on IM9, KMS-12-BM, AMO-1, and NCI-H929, in a time- and concentration-dependent manner at IC_{50}s of 75. 1, 77.2, 84.1, and 280.0 nM, respectively (Figure 1a; Supplementary Figure 1). The only exception was RPMI8226, against which >1 μM hGal9 did not have any anti-proliferative effect. As was shown by the increased number of Annexin V-positive cells in hGal9-treated cells (Figure 1b), the anti-myeloma effect of hGal9 involved the induction of apoptosis. The apoptotic induction by hGal9 was accompanied by the loss of MOMP and the processing of caspase-3, -8, and -9 (Figures 1c and d). The blockade of caspase activation by the pretreatment with either Z-VAD-FMK, a pan-caspase inhibitor, or Z-IETD-FMK, an inhibitor for caspase-8, partly prevented the cell death induction by hGal9, whereas the pretreatment with Z-LEHD-FMK, an inhibitor for caspase-9, did not protect cells from hGal9-induced cell death in KMS-12-BM and IM9 (Figure 1e and data not shown).

Cell surface binding is the prerequisite for the anti-MM activity of hGal9

The addition of 25 mM lactose completely abrogated the anti-myeloma activity of hGal9 (Figure 2a). The cell lines with stronger affinity for hGal9 are more sensitive to the anti-proliferative effect of hGal9, whereas hGal9-resistant RPMI8226 has the lowest affinity for hGal9 (Figures 2b and c).

JNK and p38 MAPK signaling pathways in the anti-myeloma effect of hGal9

Microarray analyses showed that 16 genes, including *c-jun* and *junD*, were upregulated by hGal9 in KMS-12-BM and IM9. The upregulation of *c-jun* and *junD* genes by hGla9 was confirmed by RQ-PCR (Supplementary Table 1; Supplementary Figure 2), and the upregulation of c-Jun and JunD proteins by hGal9 was also confirmed (Figure 3a). The Ingenuity pathway analysis suggested the relationship between the anti-MM effect of hGal9 and the cross-talk networks of JNK and p38 MAPK signaling pathways (Supplementary Figure 3), and, indeed, JNK and p38 were phosphorylated by treatment with hGal9 in both KMS-12-BM and IM9. hGal9 also induced H2AX phosphorylation, which is critical for apoptosis by JNK activation or p38 MAPK activation (Figure 3a).[21–24] Conversely, neither JNK nor p38 activation was observed in myeloma cell lines those are resistant to hGal9-induced cell death (Supplementary Figure 7). Next, KMS-12-BM and IM9 cells were preincubated with 20 μM JNK-inhibitor VIII and/or 20 μM SB203580 for 2 h and then treated with 100 nM hGal9 for 48 h. Neither JNK-inhibitor VIII nor SB203580 alone decreased the cell viability of two cell lines. The blockade of the JNK or p38 MAPK pathway partially eliminates the cytotoxic effect of hGal9 on both cell lines, whereas the concomitant blockade of both kinases did not further increase the number of viable cells (Figures 3b and c), indicating that the activation of the JNK and p38 MAPK pathways at least partly mediates the anti-MM activity of hGal9 in a complementary manner.

The effects of hGal9 on primary myeloma cells isolated from MM patients

We examined the effect of hGal9 on myeloma cells freshly isolated from 10 patients. Three patients were treatment-naive, five relapsed after hematopoietic stem cell transplantation, one was treated with a Bor-containing regimen, and one was with a thalidomide-containing regimen. Five had chromosome abnormality t(4;14), seven had 13q chromosomal deletion, and four had both. Two had 17p chromosomal deletion (Supplementary Table 2). More than 80% of the untreated cells remained alive, whereas the 48-h treatment with hGal9 significantly reduced the number of viable cells in a dose-dependent manner in all samples examined (Figure 4).

No cross-resistance between hGal9 and Bor in IM9 cells

IM9-Bor was approximately four times more resistant to Bor with an IC_{50} of 22.3 nM compared with parental IM9

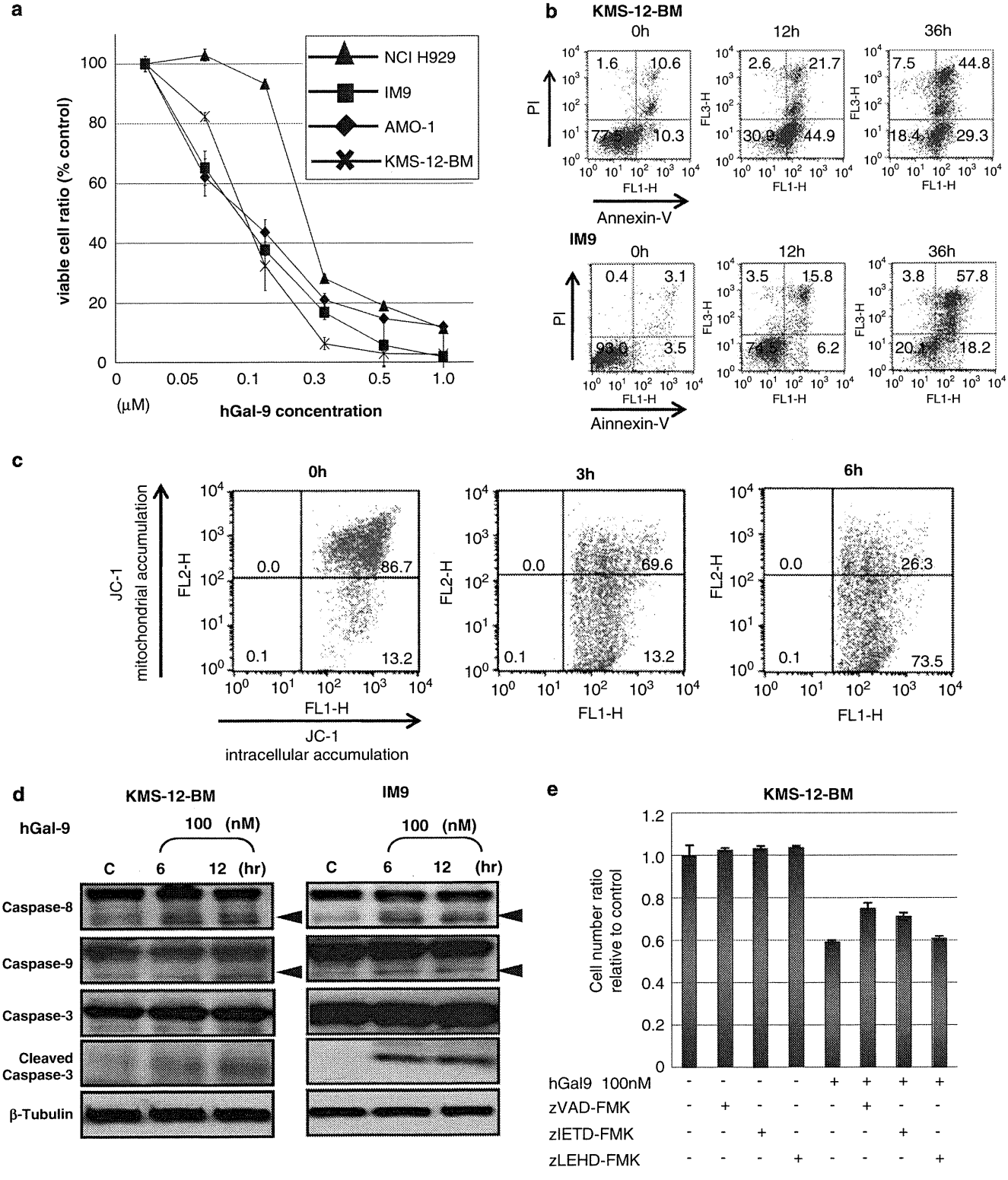

Figure 1 hGal9 inhibits cell proliferation and induces apoptosis in myeloma cell lines. (**a**) Growth-inhibitory effect of hGal9 for 48 h in MM cell lines, examined by a modified MTT assay. (**b**) Apoptosis in KMS-12-BM and IM-9 cells treated with 100 nM hGal9 for indicated period (*x* axis; Annexin-V-FITC, *y* axis; propidium iodide (PI)). (**c**) The loss of mitochondrial accumulation of JC-1 reveals the loss of MOMP by hGal9. IM9 cells were treated with 100 nM hGal9 for the periods indicated. (**d**) hGal9 activates caspase-8, -9, and -3. KMS-12-BM and IM9 cells were treated with hGal9 for the periods indicated. Arrowheads denote cleaved caspase-8 and cleaved caspase-9. (**e**) Caspase-dependent and -independent cell death induction by hGal9 in myeloma cells. KMS-12-BM cells were treated by 100 nM hGal9 for 24 h with or without the pretreatment with either by 50 μM of either zVAD-FMK, zIETD-FMK, or zLEHD-FMK for 1 h.

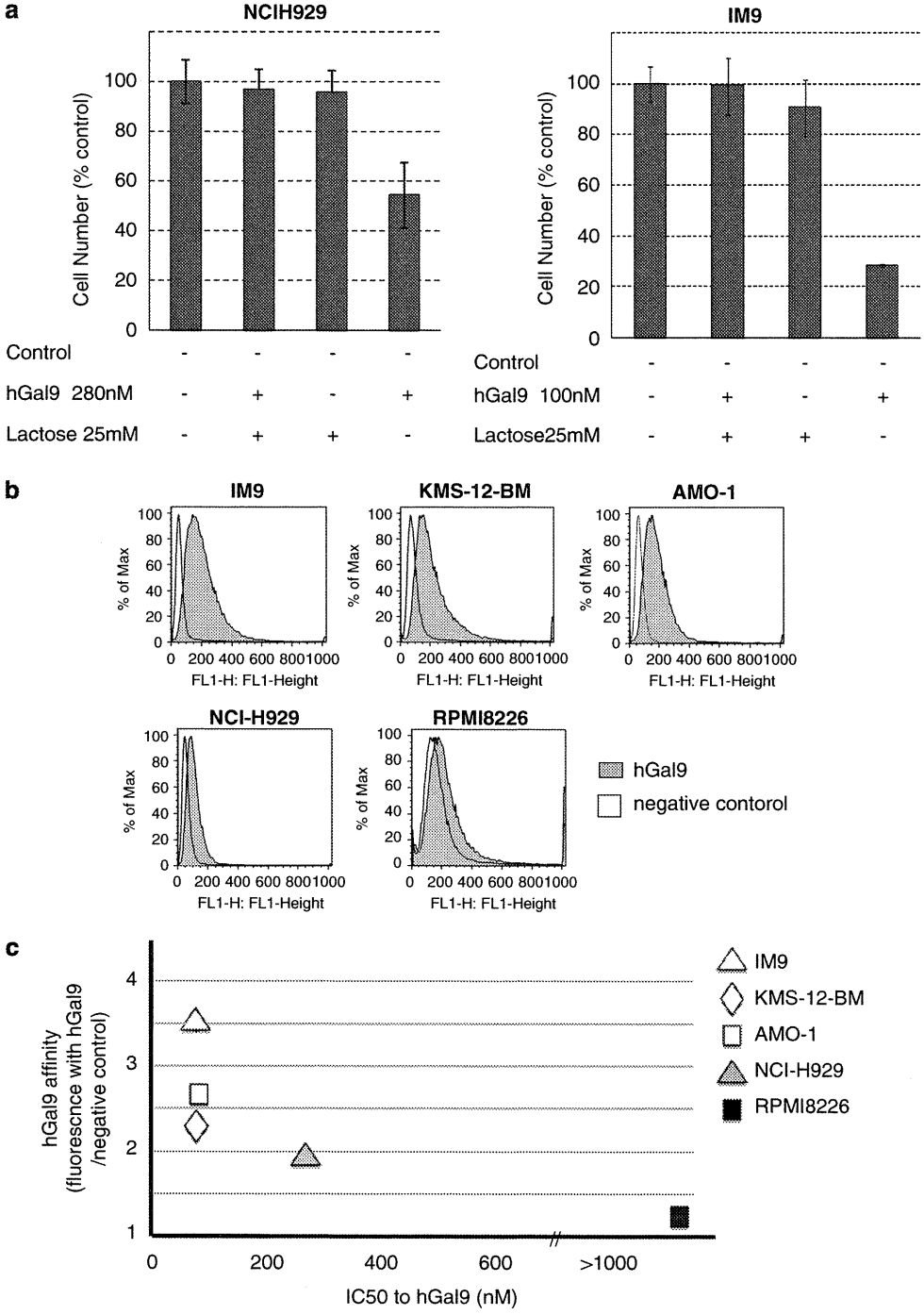

Figure 2 Cell surface binding affinity and the anti-MM activity of hGal9. (**a**) NCI-H929 and IM9 were treated with hGal9 with or without 25 mM lactose for 48 h, and the relative cell number was assessed with a modified MTT assay. (**b**) Cell surface binding affinity of hGal9. *x* axis; the degree of cell surface hGal9 binding, *y* axis; the cell number. (**c**) Relationship between cell surface hGal9 affinity and IC_{50} concentration of hGal9. The *x* axis shows IC_{50} concentrations of hGal9 for 48-h treatment, and the *y* axis shows the relative cell surface affinities of hGal9. The relative cell surface binding affinity of hGal9 was calculated by using the ratio between the median fluorescence intensity of cell surface bound biotinylated hGal9NC and that of cell surface bound negative control in individual cell lines.

with an IC_{50} of 5.4 nM. By contrast, both cell lines showed the similar cell surface binding affinity for hGal9, and hGal9 was effective without any statistically significant difference against both IM9 and IM9-Bor cells with respective IC_{50}s of 75.1 and 112.6 nM (Figures 5a and b; Supplementary Figure 4).

hGal9 inhibits the proliferation of IM9 cells in vivo

As shown in Figure 6, hGal9 treatment for 14 consecutive days significantly delayed the tumor growth of IM9 cells ($P<0.05$; Mann–Whitney *U*-test), thus constituting evidence for the direct *in vivo* anti-myeloma activity of hGal9.

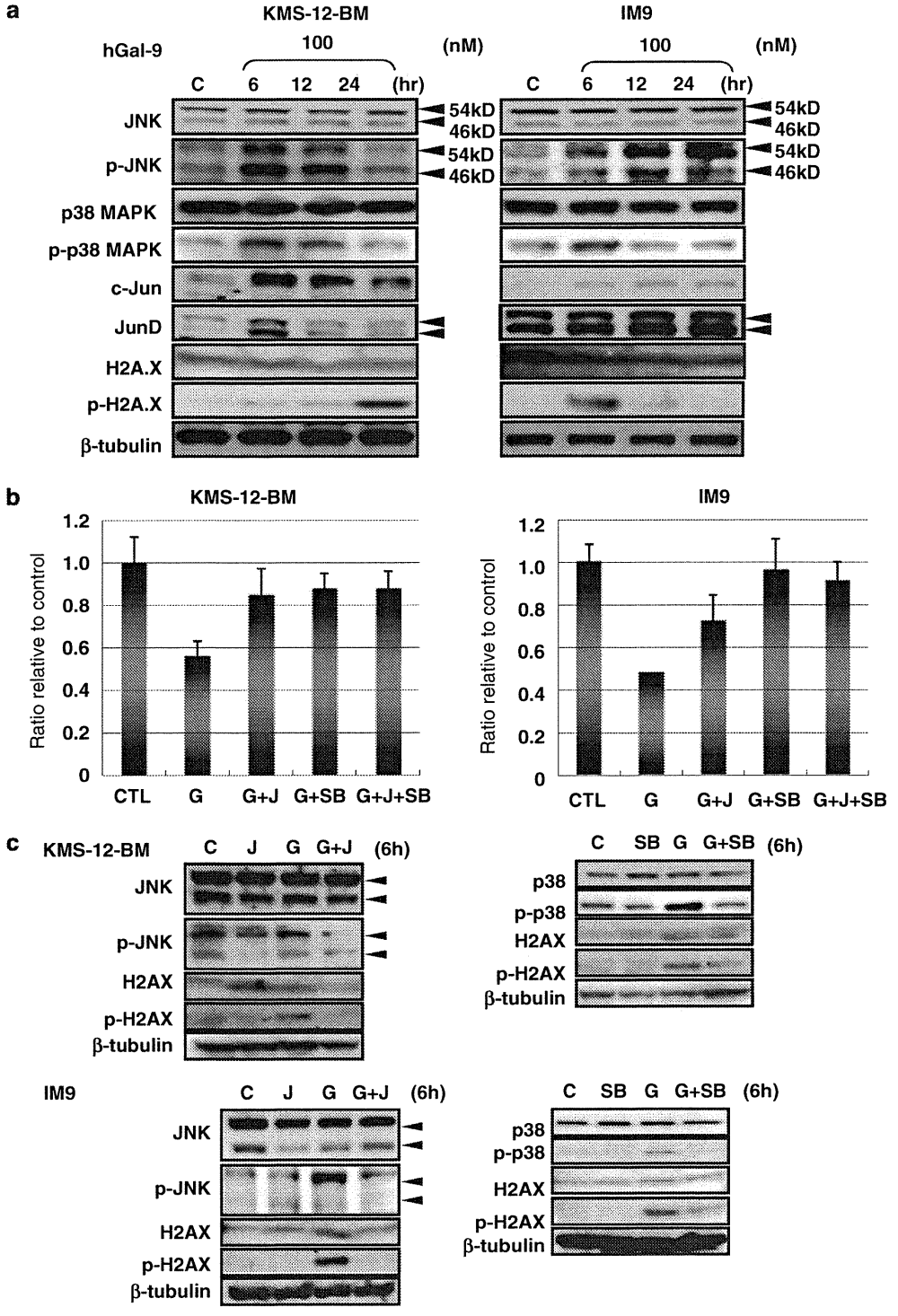

Figure 3 Activation of JNK/p38 MAP kinases in apoptosis induced by hGal9 in myeloma cell lines. (**a**) Western blot analyses in KMS-12-BM cells and IM9. (**b**) Blockade of JNK and/or p38 MAPK phosphorylation reduced hGal9 (100 nM)-induced cell death (C, control; G, hGal9; J, JNK-inhibitor VIII; SB, SB203580). (**c**) Western blot analyses. JNK-inhibitor VIII or SB203580 inhibits the activation of JNK or p38 MAPK, respectively, by hGal9 in KMS-12-BM and IM9 cells (C, control; J, JNK-inhibitor VIII; SB, SB203580; G, hGal9).

Discussion

Here, we showed that the anti-myeloma activity of hGal9 was mediated by the activation of JNK and p38 MAPK signaling pathways. Reportedly, JNK activation is one of the crucial pathways for apoptosis induction by the leading anti-MM agents such as proteasome inhibitors or IMiDs, or various new candidate agents for MM.[16,25–29] Also, various new candidate anti-MM agents, such as the histone deacetylase inhibitor PXD101, induce apoptosis by activating the p38 MAPK pathway in myeloma cells.[30–33] These findings lead us to suggest that both JNK and p38 pathways activation are the logical molecular targets for the development of new therapeutic strategies for MM. On the other hand, although earlier studies suggest that

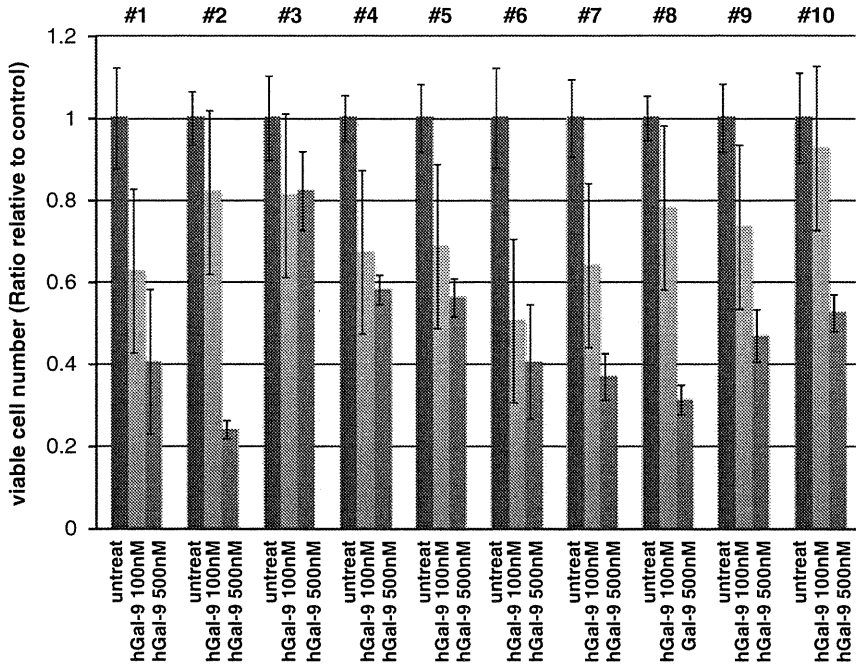

Figure 4 *In vitro* cytotoxicity of hGal9 against patient-derived myeloma cells. Cells were treated with hGal9 for 48 h and the number of viable cells was determined by direct cell counting.

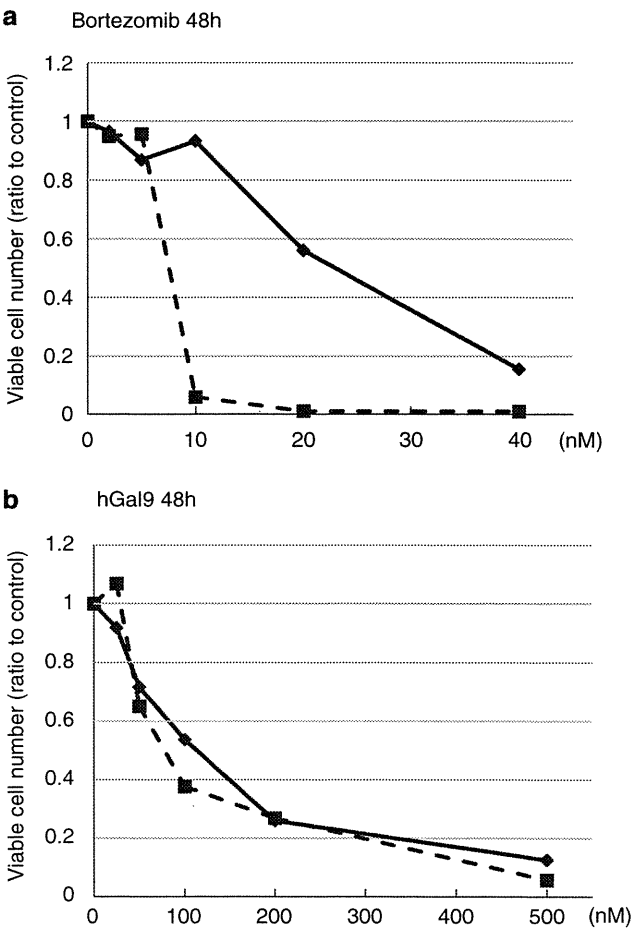

Figure 5 Effect of bortezomib or hGal9 on the IM9 or IM9-Bor. IM9 (dotted line) and IM9-Bor (solid line) were treated with bortezomib (0–40 nM) (**a**) or hGal9 (0–500 nM) (**b**) for 48 h. Ratios of viable cells were determined with a modified MTT assay.

NF-κB signaling inactivation or the activation of Ca^{2+}-calpain-caspase-1 pathway are involved in the anti-proliferative effect of hGal9 in other cancers,[13,14,34] those were not the case in the myelomas (data not shown). These indicate that, as hGal9 recognizes various β-galactosides-containing surface molecules that may differ among cell types, its primary molecular targets may also differ according to cancer type. Also, our study reveals that hGal9-induced apoptosis involves both caspase-dependent and -independent pathways, and suggests that caspase-8 activation has more dominant role than caspase-9 as the initiator caspase in cell death induced by hGal9 in myeloma cells. No specific effect of hGal9 was observed on the expression levels of Bcl-2 family protein, the crucial regulators for intrinsic apoptosis pathway, or death receptor molecules, such as Fas or DR5 (Supplementary Figure 5). Thus, we speculate that hGal9 may activate an apoptotic pathway, such as endoplasmic reticulum stress pathway, which activates JNK and p38 and then activate caspase-8 independently from classical intrinsic or extrinsic apoptosis pathway,[35] and, consequently, may activate caspase-9 and caspase-3 in cascade.

There is an urgent need for the development of new therapeutic strategies for MM patients. hGal9-induced cell death in all 10 primary human myeloma cells tested, even in cells from treatment-resistant patients with poor prognosis chromosomal abnormalities. Compared with cell lines, a higher dose of hGal9 seems to be required for killing primary myeloma cells, presumably because these cells may become quiescent and less sensitive to any cytotoxic stimuli *ex vivo*. Also, hGal9 was found to inhibit proliferation of IM9-Bor to a similar degree as that seen in bortezomib-sensitive parental IM9 cells. hGal9 was also found to be safe for mice, did not result in body weight reduction during treatment (data not shown), and did not significantly inhibit normal human CFU-GM formation (Supplementary Figure 6). Thus, hGal9 may be a new candidate nti-MM agent even for high-risk MM patients. Although the 'subcutaneous xenografted' myeloma model used in this study showed the *in vivo* bioactivity of hGal9, this model has the

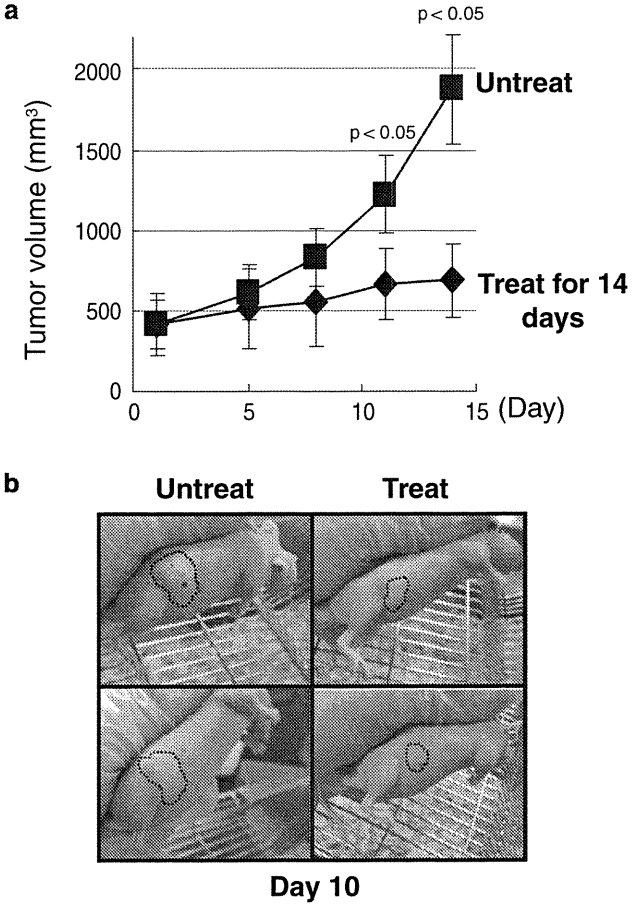

Figure 6 *In vivo* activity of hGal9. (**a**) Average tumor volumes of hGal9-untreated (only given PBS) and -treated mice during the treatment period. (**b**) Untreated IM9 inoculated nude mice (left) and those treated with hGal9 for 10 days (right).

potential limitation for recapitulating MM, which normally represents multiple tumors in systemic BM sites. It is urgently desired to explore the anti-myeloma effect of hGal9 at multiple BM sites.

In conclusion, we have shown the activity of hGal9 against myeloma cell lines and primary human MM cells both *in vitro* and *in vivo*, and that the activation of JNK/p38-H2AX pathways is involved in this anti-myeloma activity. Further clinical study of hGal9 as a new anti-MM agent thus certainly seems to be warranted.

Conflict of interest

The authors declare no conflict of interest.

Acknowledgements

This work was partly supported by Grants-in-Aid for Scientific Research from the Ministry of Education, Culture, Sports, Science, and Technology of Japan, and by grants from the Kobayashi Foundation of Innovative Cancer Chemotherapy, the Award in Aki's Memory from International Myeloma Foundation, and the Japan Leukaemia Research Fund (MT and JK).

References

1 Barondes SH, Castronovo V, Cooper DN, Cummings RD, Drickamer K, Feizi T *et al.* Galectins: a family of animal beta-galactoside-binding lectins. *Cell* 1994; **76**: 597–598.
2 Barondes SH, Cooper DN, Gitt MA, Leffler H. Galectins: structure and function of a large family of animal lectins. *J Biol Chem* 1994; **269**: 20807–20810.
3 Brewer CF. Binding and cross-linking properties of galectins. *Biochem Biophys Acta* 2002; **1572**: 255–262.
4 Wada J, Ota K, Kumar A, Wallner EI, Kanwar YS. Developmental regulation, expression, and apoptotic potential of galectin-9, a beta-galactosides binding lectin. *J Clin Invest* 1997; **99**: 2452–2461.
5 Perillo NL, Marcus ME, Baum LG. Galectins: versatile modulators of cell adhesion, cell proliferation, and cell death. *J Mol Med* 1998; **76**: 402–412.
6 Rabinovich GA. Galectins: an evolutionarily conserved family of animal lectins with multifunctional properties; a trip from the gene to clinical therapy. *Cell Death Differ* 1999; **6**: 711–721.
7 Liu FT. Galectins: a new family of regulators of inflammation. *Clin Immunol* 2000; **97**: 79–88.
8 Matsumoto R, Matsumoto H, Seki M, Hata M, Asano Y, Kanegasaki S *et al.* Human ecalectin, a variant of human galectin-9, is a novel eosinophil chemoattractant produced by T lymphocytes. *J Biol Chem* 1998; **273**: 16976–16984.
9 Seki M, Oomizu S, Sakata K, Arikawa T, Watanabe K, Ito K *et al.* Galectin-9 suppresses the generation of Th17, promotes the induction of regulatory T cells, and regulates experimental autoimmune arthritis. *Clin Immunol* 2008; **127**: 78–88.
10 Dai SY, Nakagawa R, Itoh A, Murakami H, Kashio Y, Abe H *et al.* Galectin-9 induces maturation of human monocyte-derived dendritic cells. *J Immunol* 2005; **175**: 2974–2981.
11 Kageshita T, Kashio Y, Yamauchi A, Seki M, Abedin MJ, Nishi N *et al.* Possible role of galectin-9 in cell aggregation and apoptosis of human melanoma cell lines and its clinical significance. *Int J Cancer* 2002; **99**: 809–816.
12 Lu LH, Nakagawa R, Kashio Y, Ito A, Shoji H, Nishi N *et al.* Characterization of galectin-9-induced death of Jurkat T cells. *J Biochem* 2007; **141**: 157–172.
13 Okudaira T, Hirashima M, Ishikawa C, Makishi S, Tomita M, Matsuda T *et al.* A modified version of galectin-9 suppresses cell growth and induced apoptosis of human T-cell leukemia virus type I-infected T-cell lines. *Int J Cancer* 2007; **120**: 2251–2261.
14 Makishi S, Okudaira T, Ishikawa C, Sawada S, Watanabe T, Hirashima M *et al.* A modified version of galectin-9 induces cell cycle arrest and apoptosis of Burkitt and Hodgkin lymphoma cells. *Br J Haematol* 2008; **142**: 583–594.
15 Nobumoto A, Nagahara K, Oomizu S, Katoh S, Nishi N, Takeshita K *et al.* Galectin-9 suppresses tumor metastasis by blocking adhesion to endothelium and extracellular matrices. *Glycobiology* 2008; **18**: 735–744.
16 Kiziltepe T, Hideshima T, Ishitsuka K, Ocio EM, Raje N, Catley L *et al.* JS-K, a GST-activated nitric oxide generator, induces DNA double-strand breaks, activates DNA damage response pathways, and induces apoptosis *in vitro* and *in vivo* in human multiple myeloma cells. *Blood* 2007; **110**: 709–718.
17 Kuroda J, Kamitsuji Y, Kimura S, Ashihara E, Kawata E, Nakagawa Y *et al.* Anti-myeloma effect of homoharringtonine with concomitant targeting of the myeloma-promoting molecules, Mcl-1, XIAP, and beta-catenin. *Int J Hematol* 2008; **87**: 507–515.
18 Nishi N, Itoh A, Fujiyama A, Yoshida N, Araya S, Hirashima M *et al.* Development of highly stable galectins: truncation of the linker peptide confers protease-resistance on tandem-repeat type galectins. *FEBS Lett* 2005; **579**: 2058–2064.
19 Kuroda J, Kimura S, Segawa H, Sato K, Matsumoto S, Nogawa M *et al.* p53-independent anti-tumor effects of the nitrogen-containing bisphosphonate zoledronic acid. *Cancer Sci* 2004; **95**: 186–192.
20 Kuroda J, Puthalakath H, Cragg MS, Kelly PN, Bouillet P, Huang DCS *et al.* Bim and Bad mediate imatinib-induced killing of Bcr/Abl$^+$ leukemic cells and resistance due to their loss is overcome by a BH3 Mimetic. *Proc Natl Acad Sci USA* 2006; **103**: 14907–14912.